previously (21), on the other hand, could be the key to exocytosis at the abluminal side. The importance of Ca^{2+} signaling for exocytosis has been studied in detail for nerve cells (34) and has also been shown in astrocytes (35) and adrenal chromaffin cells (36). There has been speculation that it might be a more general mechanism also found in endothelial cells (14, 37), and our results contribute to and support this hypothesis.

In summary, our studies provide evidence for CysLT-mediated vascular permeability alterations exclusively *via* $CysLT_2R$ by means of transcellular endothelial vesicle transport, which is likely mediated by oscillatory Ca^{2+} signaling. Understanding and controlling this vascular hyperpermeability response is likely to be of importance for managing the clinical response to vascular injury and perhaps for preventing post-traumatic injury edema formation. However, since there are some differences in $CysLT_2R$ expression patterns between mice and humans (13, 38, 39), caution will have to be exercised before translating this work to human vascular disorders. FJ

We thank Dr. Yves St. Pierre (University of Quebec) for kindly supplying the murine b-end.3 cells. This work was supported by Canadian Institutes of Health Research grant MOP-68930 and the Canadian Foundation for Innovation. C.D.F. holds a Tier I Canada Research Chair in Molecular, Cellular, and Physiological Medicine and is recipient of a Career Investigator Award from the Heart and Stroke Foundation of Ontario. M.P.W.M. was supported by the German Academy of Sciences Leopoldina with the German Federal Ministry of Education and Research, BMBF-LPD 9901/8-132.

REFERENCES

1. Aller, M. A., Arias, J. L., Sánchez-Patán, F., and Arias, J. (2006) The inflammatory response: an efficient way of life. *Med. Sci. Monit.* **12,** RA225–234
2. Choileain, N. N., and Redmond, H. P. (2006) Cell response to surgery. *Arch. Surg.* **141,** 1132–1140
3. Shiels, I. A., Taylor, S. M., and Fairlie, D. P. (2000) Cell phenotype as a target of drug therapy in chronic inflammatory diseases. *Med. Hypotheses* **54,** 193–197
4. Funk, C. D. (2001) Prostaglandins and leukotrienes: advances in eicosanoid biology. *Science* **294,** 1871–1875
5. Ciana, P., Fumagalli, M., Trincavelli, M. L., Verderio, C., Rosa, P., Lecca, D., Ferrario, S., Parravicini, C., Capra, V., Gelosa, P., Guerrini, U., Belcredito, S., Cimino, M., Sironi, L., Tremoli, E., Rovati, G. E., Martini, C., and Abbracchio, M. P. (2006) The orphan receptor GPR17 identified as a new dual uracil nucleotides/cysteinyl-leukotrienes receptor. *EMBO J.* **25,** 4615–4627
6. Funk, C. D. (2005) Leukotriene modifiers as potential therapeutics for cardiovascular disease. *Nat. Rev. Drug Discov.* **4,** 664–672
7. Lötzer, K., Funk, C. D., and Habenicht, A. J. (2005) The 5-lipoxygenase pathway in arterial wall biology and atherosclerosis. *Biochim. Biophys. Acta* **1736,** 30–37
8. Helgadottir, A., Manolescu, A., Thorleifsson, G., Gretarsdottir, S., Jonsdottir, H., Thorsteinsdottir, U., Samani, N. J., Gudmundsson, G., Grant, S. F., Thorgeirsson, G., Sveinbjornsdottir, S., Valdimarsson, E. M., Matthiasson, S. E., Johannsson, H., Gudmundsdottir, O., Gurney, M. E., Sainz, J., Thorhallsdottir, M., Andresdottir, M., Frigge, M. L., Topol, E. J., Kong, A., Gudnason, V., Hakonarson, H., Gulcher, J. R., and Stefansson, K. (2004) The gene encoding 5-lipoxygenase activating protein confers risk of myocardial infarction and stroke. *Nat. Genet.* **36,** 233–239
9. Dwyer, J. H., Allayee, H., Dwyer, K. M., Fan, J., Wu, H., Mar, R., Lusis, A. J., and Mehrabian, M. (2004) Arachidonate 5-lipoxygenase promoter genotype, dietary arachidonic acid, and atherosclerosis. *N. Engl. J. Med.* **350,** 29–37
10. Hui, Y., Cheng, Y., Smalera, I., Jian, W., Goldhahn, L., Fitzgerald, G. A., and Funk, C. D. (2004) Directed vascular expression of human cysteinyl leukotriene 2 receptor modulates endothelial permeability and systemic blood pressure. *Circulation* **110,** 3360–3366
11. Jiang, W., Hall, S. R., Moos, M. P. W., Cao, R. Y., Ishii, S., Ogunyankin, K. O., Melo, L. G., and Funk, C. D. (2008) Endothelial cysteinyl leukotriene 2 receptor ($CysLT_2R$) expression mediates myocardial ischemia-reperfusion injury. *Am. J. Pathol.* **172,** 592–602
12. Beller, T. C., Maekawa, A., Friend, D. S., Austen, K. F., and Kanaoka, Y. (2004) Targeted gene disruption reveals the role of the cysteinyl leukotriene 2 receptor in increased vascular permeability and in bleomycin-induced pulmonary fibrosis in mice. *J. Biol. Chem.* **279,** 46129–46134
13. Hui, Y., Yang, G., Galczenski, H., Figueroa, D. J., Austin, C. P., Copeland, N. G., Gilbert, D. J., Jenkins, N. A., and Funk, C. D. (2001) The murine cysteinyl leukotriene 2 (CysLT2) receptor. cDNA and genomic cloning, alternative splicing, and *in vitro* characterization. *J. Biol. Chem.* **276,** 47489–47495
14. Mehta, D., and Malik, A. B. (2006) Signaling mechanisms regulating endothelial permeability. *Physiol. Rev.* **86,** 279–367
15. McCafferty, D. M., Craig, A. W., Senis, Y. A., and Greer, P. A. (2002) Absence of Fer protein-tyrosine kinase exacerbates leukocyte recruitment in response to endotoxin. *J. Immunol.* **168,** 4930–4935
16. Warren, M., Huizar, J. F., Shvedko, A. G., and Zaitsev, A. V. (2007). Spatiotemporal relationship between intracellular Ca2+ dynamics and wave fragmentation during ventricular fibrillation in isolated blood-perfused pig hearts. *Circ. Res.* **101,** e90–e101
17. Fleming, I., Fisslthaler, B., and Busse, R. (1995) Calcium signaling in endothelial cells involves activation of tyrosine kinases and leads to activation of mitogen-activated protein kinases. *Circ. Res.* **76,** 522–529
18. Gericke, M., Droogmans, G., and Nilius, B. (1993) Thapsigargin discharges intracellular calcium stores and induces transmembrane currents in human endothelial cells. *Pflügers Arch.* **422,** 552–557
19. El-Mestrah, M., and Kan, F. W. (1999) Ultrastructural and ultracytochemical features of secretory granules in the ampullary epithelium of the hamster oviduct. *Anat. Rec.* **255,** 227–239
20. Huang, Q., Xu, W., Ustinova, E., Wu, M., Childs, E., Hunter, F., and Yuan, S. (2003) Myosin light chain kinase-dependent microvascular hyperpermeability in thermal injury. *Shock* **20,** 363–368
21. Lötzer, K., Spanbroek, R., Hildner, M., Urbach, A., Heller, R., Bretschneider, E., Galczenski, H., Evans, J. F., and Habenicht, A. J. (2003) Differential leukotriene receptor expression and calcium responses in endothelial cells and macrophages indicate 5-lipoxygenase-dependent circuits of inflammation and atherogenesis. *Arterioscler. Thromb. Vasc. Biol.* **23,** e32–36
22. Koopman, W. J., Scheenen, W. J., Schoolderman, L. F., Cruijsen, P. M., Roubos, E. W., and Jenks, B. G. (2001) Intracellular calcium buffering shapes calcium oscillations in Xenopus melanotropes. *Pflügers Arch.* **443,** 250–256
23. Predescu, D., Vogel, S. M., and Malik, A. B. (2004) Functional and morphological studies of protein transcytosis in continuous endothelia. *Am. J. Physiol. Lung Cell. Mol. Physiol.* **287,** L895–L901
24. Fredholm, B. B., Hökfelt, T., and Milligan, G. (2007) G-protein-coupled receptors: an update. *Acta Physiol.* **190,** 3–7
25. Casillan, A. J., Gonzalez, N. C., Johnson, J. S., Steiner, D. R., and Wood, J. G. (2003) Mesenteric microvascular inflammatory responses to systemic hypoxia are mediated by PAF and LTB4. *J. Appl. Physiol.* **94,** 2313–2322
26. Laemmel, E., Genet, M., Le Goualher, G., Perchant, A., Le Gargasson, J. F., and Vicaut, E. (2004) Fibered confocal fluorescence microscopy (Cell-viZio) facilitates extended imaging in the field of microcirculation. A comparison with intravital microscopy. *J. Vasc. Res.* **41,** 400–411
27. Ferri, L. E., Pascual, J., Seely, A. J., Chaudhury, P., and Christou, N. V. (2002) Soluble L-selectin attenuates tumor necrosis factor-alpha-mediated leukocyte adherence and vascular permeability:

a protective role for elevated soluble L-selectin in sepsis. *Crit. Care Med.* **30,** 1842–1847
28. Lominadze, D., Roberts, A. M., Tyagi, N., Moshal, K. S., and Tyagi, S. C. (2006) Homocysteine causes cerebrovascular leakage in mice. *Am. J. Physiol. Heart Circ. Physiol.* **290,** H1206–1213
29. Ghitescu, L., Fixman, A., Simionescu, M., and Simionescu, N. (1986) Specific binding sites for albumin restricted to plasmalemmal vesicles of continuous capillary endothelium: receptor-mediated transcytosis. *J. Cell Biol.* **102,** 1304–11
30. Hashizume, K., and Black, K. L. (2002) Increased endothelial vesicular transport correlates with increased blood-tumor barrier permeability induced by bradykinin and leukotriene C4. *J. Neuropathol. Exp. Neurol.* **61,** 725–735
31. Nothacker, H. P., Wang, Z., Zhu, Y., Reinscheid, R. K., Lin, S. H., and Civelli, O. (2000) Molecular cloning and characterization of a second human cysteinyl leukotriene receptor: discovery of a subtype selective agonist. *Mol. Pharmacol.* **58,** 1601–1608
32. Van Nieuw Amerongen, G. P., Draijer, R., Vermeer, M. A., and van Hinsbergh, V. W. (1998) Transient and prolonged increase in endothelial permeability induced by histamine and thrombin: role of protein kinases, calcium, and RhoA. *Circ. Res.* **83,** 1115–1123
33. Bates, D. O., Hillman, N. J., Williams, B., Neal, C. R., and Pocock, T. M. (2002) Regulation of microvascular permeability by vascular endothelial growth factors. *J. Anat.* **200,** 581–597
34. Rusakov, D. A. (2006) Ca2+-dependent mechanisms of presynaptic control at central synapses. *Neuroscientist* **12,** 317–326
35. Chen, X. K., Xiong, Y. F., and Zhou, Z. (2006) "Kiss-and-run" exocytosis in astrocytes. *Neuroscientist* **12,** 375–378
36. García, A. G., García-De-Diego, A. M., Gandía, L., Borges, R., and García-Sancho, J. (2006) Calcium signaling and exocytosis in adrenal chromaffin cells. *Physiol. Rev.* **86,** 1093–1131
37. Oheim, M., Kirchhoff, F., and Stühmer, W. (2006) Calcium microdomains in regulated exocytosis. *Cell Calcium* **40,** 423–439
38. Heise, C. E., O'Dowd, B. F., Figueroa, D. J., Sawyer, N., Nguyen, T., Im, D. S., Stocco, R., Bellefeuille, J. N., Abramovitz, M., Cheng, R., Williams, D. L. Jr., Zeng, Z., Liu, Q., Ma, L., Clements, M. K., Coulombe, N., Liu, Y., Austin, C. P., George, S. R., O'Neill, G.P., Metters, K. M., Lynch, K. R., and Evans, J. F. (2000) Characterization of the human cysteinyl leukotriene 2 receptor. *J. Biol. Chem.* **275,** 30531–30536
39. Ogasawara, H., Ishii, S., Yokomizo, T., Kakinuma, T., Komine, M., Tamaki, K., Shimizu, T., and Izumi, T. (2002) Characterization of mouse cysteinyl leukotriene receptors mCysLT1 and mCysLT2: differential pharmacological properties and tissue distribution. *J. Biol. Chem.* **277,** 18763–18768

Received for publication May 9, 2008.
Accepted for publication August 14, 2008.

Am J Physiol Cell Physiol 292: C2141–C2149, 2007.
First published January 10, 2007; doi:10.1152/ajpcell.00295.2006.

β-Defensin overexpression induces progressive muscle degeneration in mice

Yasuhiro Yamaguchi,[1,3,4] Takahide Nagase,[2] Tetsuji Tomita,[1] Kyoko Nakamura,[4] Shigetomo Fukuhara,[4] Tomokazu Amano,[3] Hiroshi Yamamoto,[1] Yukie Ide,[5] Misao Suzuki,[6] Shinji Teramoto,[1] Tomoichiro Asano,[3] Kenji Kangawa,[7] Naomi Nakagata,[5] Yasuyoshi Ouchi,[1] and Hiroki Kurihara[3,4]

Departments of [1]Geriatric Medicine, [2]Respiratory Medicine, and [3]Physiological Chemistry and Metabolism, Graduate School of Medicine, The University of Tokyo, Bunkyo-ku, Tokyo; [4]Division of Integrative Cell Biology, Department of Embryogenesis, Institute of Molecular Embryology and Genetics, and Divisions of [5]Reproductive Engineering and [6]Transgenic Technology, Center for Animal Resources and Development, Kumamoto University, Kumamoto-shi, Kumamoto; and [7]Department of Biochemistry, National Cardiovascular Center Research Institute, Suita-ku, Osaka, Japan

Submitted 27 May 2006; accepted in final form 4 January 2007

Yamaguchi Y, Nagase T, Tomita T, Nakamura K, Fukuhara S, Amano T, Yamamoto H, Ide Y, Suzuki M, Teramoto S, Asano T, Kangawa K, Nakagata N, Ouchi Y, Kurihara H. β-Defensin overexpression induces progressive muscle degeneration in mice. *Am J Physiol Cell Physiol* 292: C2141–C2149, 2007. First published January 10, 2007; doi:10.1152/ajpcell.00295.2006.—Defensins comprise a family of cationic antimicrobial peptides characterized by conserved cysteine residues. They are produced in various organs including skeletal muscle and are identified as key elements in the host defense system as potent effectors. At the same time, defensins have potential roles in the regulation of inflammation and, furthermore, can exert cytotoxic effects on several mammalian cells. Here, we developed transgenic mice overexpressing mouse β-defensin-6 to explore the pathophysiological roles of the defensin family as a novel mediator of inflammatory tissue injury. Unexpectedly, the transgenic mice showed short lifespan, poor growth, and progressive myofiber degeneration with functional muscle impairment, predominant centronucleated myofibers, and elevated serum creatine kinase activity, as seen in human muscular dystrophy. Furthermore, some of the transgenic myofibers showed IκBα accumulation, which would be related to the myofiber apoptosis of limb-girdle muscular dystrophy type 2A. The present findings may unravel a concealed linkage between the innate immune system and the pathophysiology of degenerative diseases.

muscular dystrophy; innate immunity; NF-κB

ANTIMICROBIAL PEPTIDES have emerged as a part of the host defense mechanism in animals and plants (16, 29). Defensins comprise a family of mammalian cationic antimicrobial peptides, and α-, β-, and θ-defensin subfamily members exist that conserve three specific disulfide pairings. They are produced by leukocytes and various types of epithelial cells constitutively or in response to microbial signals and inflammatory cytokines (4, 9, 10, 14, 15).

While the immune response is indispensable for the survival of humans, the chronic inflammatory response is harmful and leads to various common disorders. In addition to the potent antimicrobial effects, defensins could act on diverse immune cells and epithelial cells through CCR6, Toll-like receptor-4 (TLR4), or other mechanisms, regulating the whole immune response (5, 23, 26, 37, 40, 41). Furthermore, they exert cytotoxic effects on mammalian cells themselves (18). α-Defensin causes cell lysis of variable cultured cells through the permeabilization of cell membrane (19) and subsequent DNA injury (11, 18). Although little information had been reported regarding β-defensin cytotoxicity (21, 23), treatment of mouse blastocysts with human β-defensin-2 (hBD-2) led to their degeneration and death (28). So some participation of the defensin family would be likely in the pathogenic immune response of various diseases (32).

Recently, we identified mouse β-defensin-6 (mBD-6), a β-defensin subfamily member expressed in skeletal muscle (39). mBD-6 expression was also augmented by bacterial endotoxin, perhaps under the regulation of the NF-κB pathway like hBD-2 and mouse β-defensin-3 (3). To explore the novel effects of this molecule, we generated transgenic mice overexpressing mBD-6 constitutively. Here, we show that the dysregulated β-defensin expression resulted in extensive myofiber degeneration, reminiscent of human muscular dystrophy.

Muscular dystrophy is an inherited disorder characterized by progressive muscle degeneration. The most common form, Duchenne muscular dystrophy, is caused by mutations in the dystrophin gene, and other causative molecules like dystroglycan and sarcoglycan organize dystrophin-glycoprotein complex binding to laminin (6, 17, 30). Another form of muscular dystrophy, limb-girdle muscular dystrophy type 2A (LGMD2A), has proved to be due to the defects of calpain-3, a proteolytic enzyme (24, 31, 35). While the identification of responsible genes for muscular dystrophy has improved, the pathogenic mechanisms are not clear enough to date. Multiple factors, including immune response, are related to the pathophysiology of muscular dystrophy (33). The present finding may give a clue to the novel involvement of innate immunity in degenerative diseases like muscular dystrophy.

MATERIALS AND METHODS

Generation of transgenic mouse. The transgene was constructed by inserting the mBD-6 cDNA 3′ downstream of the chicken β-actin promoter in the pCAGGS plasmid (a gift from J. Miyazaki) (22). The excised transgene was microinjected into fertilized C57BL6/J mouse oocytes. The genomic DNA was isolated from the mice tail and analyzed by Southern blotting and/or PCR. On Southern blot analysis, the genomic DNA was digested with *BglII*, resolved on 1.0% agarose gel, and transferred to the membrane. A 250-bp fragment containing the second exon of mBD-6 was labeled by [^{32}P]dCTP using a random primed DNA labeling kit (Roche). The labeled probe was hybrid-

Address for reprint requests and other correspondence: Y. Ouchi, Dept. of Geriatric Medicine, Graduate School of Medicine, The Univ. of Tokyo, 7-3-1 Hongo, Bunkyo-ku, Tokyo, 113-0033, Japan (e-mail: youchi-tky@umin.ac.jp).

The costs of publication of this article were defrayed in part by the payment of page charges. The article must therefore be hereby marked "*advertisement*" in accordance with 18 U.S.C. Section 1734 solely to indicate this fact.

ized to the membrane using ExpresHyb (Clontech). PCR was performed using the primers spanning mBD-6 cDNA (forward primer, 5′-GGTTATTGTGCTGTCTCATC-3′; reverse primer, 5′-ATTTGTGAGCCAGGGCATTG-3′). The PCR condition was 94°C for 40 s, 60°C for 30 s, and 72°C for 60 s, carried out for 35 cycles. The one line, Tg(CAG-mBD6)1 mice, was maintained on ICR mice, and the other line, Tg(CAG-mBD6)2 mice, was maintained on C57BL6/J mice. The immunohistochemical analysis was performed on Tg(CAG-mBD6)1 mice after they were backcrossed to the C57BL6/J strain. Animal care and use in our laboratory were in strict accordance with the guidelines for animal and recombinant DNA experiments put forth by Kumamoto University and The University of Tokyo. The experiment was approved by the Committee for Animal Resources in Kumamoto University and by the University of Tokyo.

RT-PCR. Total RNA was isolated from the skeletal muscle using ISOGEN (Nippon gene). Five micrograms of each sample were reverse-transcribed using SuperscriptII (Gibco-BRL). To detect the expression of transgene, we designed a forward primer from the mBD-6 first exon (5′-ACCATGAAGATCCATTACCTG-3′) and a reverse primer from the rabbit β-globin (5′-ATTTGTGAGCCAGGGCATTG-3′), and we performed a real-time PCR reaction using the Fluorescent Quantitative Detection System Version 3.02 (LineGene).

Antiserum preparation. The putative mature peptide composed of the COOH-terminal 40 amino acids of mBD-6 was chemically synthesized at the Peptide Institute (Minoh, Japan), as previously described (39). The anti-mBD-6 rabbit serum was prepared at the Peptide Institute using this synthetic mBD-6 peptide, conjugated to keyhole limpet hemocyanin, and injected into rabbits.

Isolation of mBD-6 peptide. We followed the procedure described by Valore et al. (36). Frozen skeletal muscle was homogenized in ISOGEN (Nippon gene), and the protein was extracted according to the manufacturer's protocol. Protein pellets were incubated overnight in 5% acetic acid at 4°C, and the dissolved proteins were neutralized with 10% NH_3. These protein solutions were separated on Tris-glycine SDS-PAGE and transferred onto polyvinylidene difluoride membrane. The membrane was probed with anti-mBD-6 rabbit serum, followed by a peroxidase-conjugated anti-rabbit IgG antibody (ICN), and visualized using the Enhanced Chemiluminescence Plus System (Amersham Pharmacia Biotech).

Evaluation of muscle strength. We evaluated muscle strength by measuring the time during which mice could hang down from a stainless steel lattice. The procedure was repeated twice for each mouse, and the better record was indicated.

Evans blue dye staining and measurement of serum creatine kinase activity. We performed the intraperitoneal injection of 10 mg/ml Evans blue dye solution of phosphate-buffered saline (PBS) (0.1 ml/10 g body wt) on 2-mo-old Tg1 mice and wild-type mice. The skeletal muscle samples were removed 16 h after the injection. The frozen 10-μm sections were fixed in acetone for 1 min and observed under a fluorescence microscope. Serum creatine kinase (CK) activity was measured at SRL (Tachikawa, Japan), a commercial laboratory.

Tissue preparation and immunohistochemistry. Skeletal muscle samples were removed and frozen in isopentane chilled in liquid nitrogen. The frozen 10-μm sections were processed for hematoxylin and eosin staining or immunohistochemical analysis. For the immunohistochemistry, the sections were fixed in acetone for 5 min and probed with the following primary antibodies: anti-dystrophin for COOH terminus (C-20) (Santa Cruz), anti-α-dystroglycan for internal core part (E-21) (Santa Cruz), anti-laminin-α2 chain (LSL), anti-neural cell adhesion molecule (Chemicon), anti-IκBα (Santa Cruz), anti-cleaved-caspase-3 (Trevigen), and anti-calpain-3 antibody (a gift from H. Sorimachi).

Statistics. Comparison of the body weights or serum CK activity was made with Student's *t*-test. Values of $P < 0.05$ were considered significant.

RESULTS

Generation of transgenic mice overexpressing mBD-6. To achieve broad and high expression of mBD-6, a cDNA fragment encoding mBD-6 was connected to the 3′-end of the chicken β-actin promoter flanked with a cytomegalovirus immediate-early enhancer (Fig. 1*A*). While six founder transgenic mice were identified using PCR and Southern blot analysis, the transgene was transmitted to germline in two lines. On Southern blot analysis, the one line, Tg(CAG-mBD6)1, was estimated to harbor several copies of the transgenes because of multiple extra bands, including a 2.0-kb DNA fragment corresponding to the full-length transgene size, while the wildtype genomic DNA showed two copies of the 1.4-kb intrinsic mBD-6 gene and a more faint 3.2-kb band perhaps composed

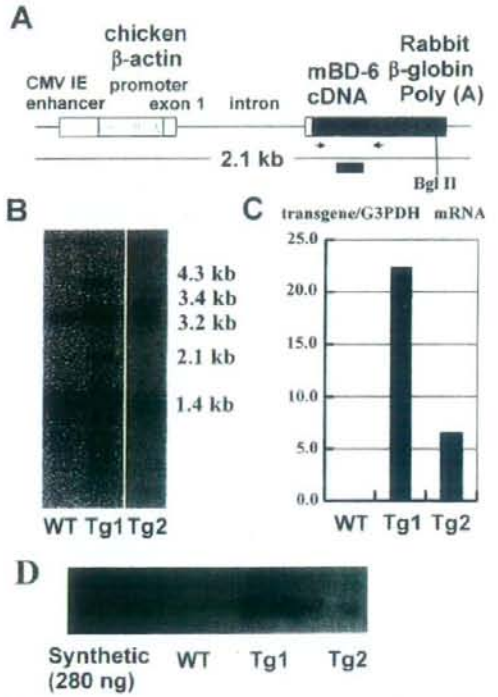

Fig. 1. Mouse β-defensin-6 (mBD-6) transgene expression. *A*: schematic description of the mBD-6 transgene fragment used to generate transgenic mice. A human cytomegalovirus immediate-early (CMV-IE) enhancer is linked to the chicken β-actin promoter, followed by its first exon and intron. In addition, a rabbit β-globin poly (A) sequence is located downstream from the mBD-6 cDNA. Black bar indicates probe of second exon of mBD-6 for Southern blot analysis in *B*. Arrows indicate the primers for RT-PCR of mBD-6 transgene. *B*: Southern blot analysis of the *Bgl*II-digested genomic DNA from Tg(CAGmBD6)1 mice (Tg1) and Tg(CAGmBD6)2 mice (Tg2). Wildtype genomic DNA showed two copies of the 1.4-kb intrinsic mBD-6 gene, and the more faint 3.2-kb band is perhaps composed of the mBD-6 pseudogene. Tg1 showed multiple extra bands, including a 2.1-kB DNA fragment corresponding to the full-length transgene size, while Tg2 showed a single 3.4-kb extra band. *C*: RT-PCR of mBD-6 transgene mRNA. The transgene-specific RT-PCR indicated transgene expression in skeletal muscle of Tg1 and Tg2. G3PDH, glyceraldehyde-3-phosphate dehydrogenase. *D*: Western blot analysis of mBD-6 peptide extracted from skeletal muscle; 280 ng of synthetic mBD-6 peptide composed of 40 NH_2-terminal residues were used as standard. mBD-6 peptide was detected in the extracts from Tg1 and Tg2 skeletal muscle but not from the wild-type mice (WT).

of the mBD-6 pseudogene. The other line, Tg(CAG-mBD6)2, was estimated to harbor a single copy because of the single 3.4-kb extra band (Fig. 1*B*). Tg(CAG-mBD6)1 and Tg(CAG-mBD6)2 mice will be referred to as Tg1 mice and Tg2 mice, respectively.

In both lines, transgene expression was detected in the skeletal muscle by RT-PCR using the primers from mBD-6 cDNA and rabbit β-globin cDNA (Fig. 1, *A* and *B*). Tg1 mice showed 3.4 times higher expression of the transgene than Tg2 mice. Western blot analysis could detect mBD-6 peptide in the extracts from Tg1 and Tg2 skeletal muscle, and the expression level was also low in Tg2 mice (Fig. 1*C*). In wild-type mice, the mBD-6 signal was not detected by Western blot analysis under the same experimental condition. Immunohistochemical analysis of the mBD-6 peptide showed the mBD-6 peptide stored in the cytoplasmic granules in some skeletal muscle myofibers of Tg1 mice.

Tg(CAG-mBD6) mice develop muscle degeneration. At birth, Tg1 and Tg2 mice were indistinguishable from their wild-type littermates. By 6 wk of age, poor growth of Tg1 mice became evident, and at 8 wk of age, both the male and female body weights of Tg1 mice were significantly lower than those of their wild-type littermates ($P < 0.01$) (Fig. 2*A*). The mean body weight of Tg1 mice was ~80% that of their wildtype littermates. They showed contracted stiff limbs and progressive kyphosis by 6 mo of age (Fig. 2*B*). Most of Tg1 mice died before 11 mo of age. The short lifespan of Tg1 mice was more evident after they were backcrossed to the C57BL6/J strain. Many of the Tg1 mice died before 8 mo, and no mice backcrossed to the C57BL6/J strain lived for >1 yr. We could not clarify the specific cause of Tg1 mouse death except severe loss of body weight. Although the other transgenic line, Tg2, did not reveal so prominently poor growth or kyphosis, 6-mo-old Tg2 male mice also showed significantly lower body weights than wild-type littermates. Tg2 mice lived for >12 mo.

Regarding the decreased body weight, we evaluated the food intake of 5-wk-old Tg1 mice. The food intake of Tg1 mice was 3.31 ± 0.12 g/day, which was significantly lower than the food intake of the wild-type littermates, which was 4.00 ± 0.29 g/day ($P < 0.05$).

Because progressive kyphosis is a prominent feature caused by functional impairment of skeletal muscle, we evaluated the muscle strength of Tg1 mice by hanging them from a stainless steel lattice. Two-month-old Tg1 mice dropped in a significantly shorter time from the lattice, indicating muscle weakness in Tg1 mice. While most of the wild-type littermates hung for >120 s, significantly more Tg1 mice dropped before 60 s ($P < 0.01$) (Fig. 3).

Hematoxylin and eosin staining of skeletal muscle revealed degenerative myofibers, infiltration of mononuclear cells, and some centronucleated myofibers in 4-wk-old Tg1 mice. After 8 wk of age, centronucleated myofibers became much more predominant, and faintly stained necrotic myofibers, basophilic regenerating myofibers, and fiber splitting were frequently encountered. The myofibers also showed prominent differences in size (Fig. 3). These features were observed in all skeletal muscles examined, including gastrocnemius muscles, anterior tibial muscles, soleus muscles, diaphragm, and muscles of the back. Meanwhile, no histological abnormalities were noted in 20-day-old Tg1 mice (Fig. 4). The other transgenic line, Tg2, revealed no histological abnormalities in skeletal muscle until ~6 mo of age. However, 1-yr-old Tg2 mice showed a few faintly stained degenerative myofibers in various muscles. The number of centronucleated myofibers in 1-yr-old Tg2 mice was also significantly increased compared with wild-type mice of the same age (2.5 ± 0.5 vs. 0.2 ± 0.1%).

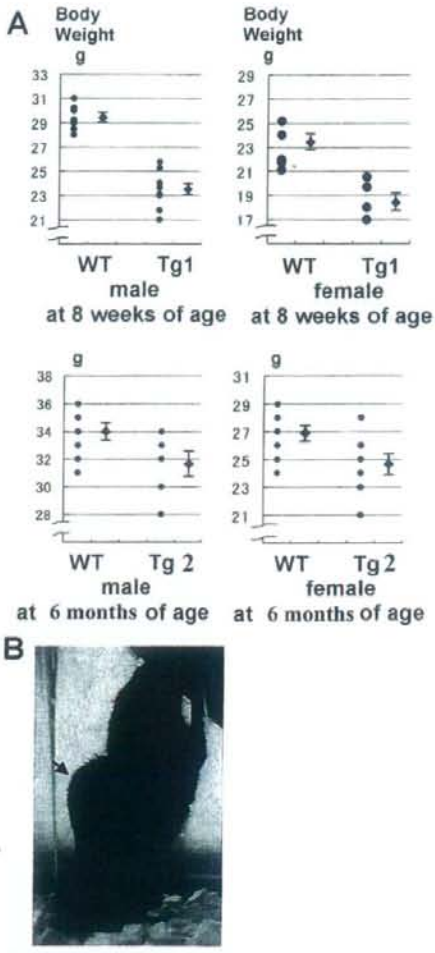

Fig. 2. Poor growth and progressive kyphosis of Tg1 mice. *A*: comparison of body weights between Tg and WT mice. Each circular point (●) indicates the measured individual body weight. Mean values (◆) ± SD are also shown. Both the male and female body weights of Tg mice were significantly lower than those of WT. *B*: photograph of 6-mo-old Tg1 mouse. Arrow indicates kyphosis.

We measured serum CK activity in 3-mo-old Tg-1 mice and their wild-type littermates because the measurement of serum CK activity is used clinically to ascertain muscular damage. Tg1 mice showed significantly higher serum CK activity than the wild-type littermates ($P < 0.01$) (Fig. 5*A*). Evans blue dye labeling also detected more clearly the damaged myofibers, with increased membrane permeability in Tg1 mice and aged 1-yr-old Tg2 mice (Fig. 5*B*).

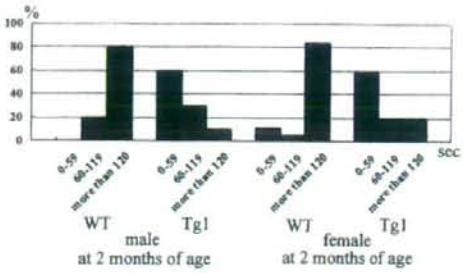

Fig. 3. Evaluation of muscle strength of Tg1 mice. We evaluated muscle strength by measuring the time during which mice could hang down from a stainless steel lattice. Graph shows percentage of mice that could hang down for the indicated time. While most of the WT littermates hung down for >120 s, many of Tg1 mice dropped before 60 s.

Evaluation of causative proteins of muscular dystrophy. These skeletal muscle phenotypes caused by mBD-6 overexpression are reminiscent of muscular dystrophies, characterized by progressive myofiber degeneration. In mBD-6 transgenic mice, organization of the dystrophin-glycoprotein complex was not different from that of wild-type littermates on the immunohistochemistry of dystrophin, α-dystroglycan, and laminin (Fig. 6). Likewise, the expression of calpain-3 showed no abnormality in mBD-6 transgenic mice (Fig. 6).

Immunohistochemical abnormalities of the transgenic myofibers. To investigate the molecular mechanisms of myofiber degeneration, we evaluated the conserved immunohistochemical features of young Tg1 mice and aged Tg2 mice.

In 1-mo-old Tg1 mice, many myofibers showed a high level of expression of neural cell adhesion molecule (NCAM). Also, in Tg2 mice, many NCAM-positive myofibers were detected at 11–12 mo of age, while their wild-type littermates of the same age showed only a few NCAM-positive myofibers (Fig. 7*A*). Although denervated myofibers upregulate NCAM expression, the number and morphology of motor neurons were not different between the Tg1 mice and their wild-type littermates (Fig. 8). We also examined the distribution of IκBα in Tg1 and Tg2 mice. We detected the accumulation of IκBα in many myofibers of 1-mo-old Tg1 mice and 12-mo-old Tg2 mice (Fig. 7*B*), as reported in LGMD2A patients (2). We also evaluated the apoptotic features of IκBα-positive myofibers in transgenic mice. In the staining of serial sections, some of the IκBα-positive myofibers showed the signal of cleaved caspase-3, the active form of caspase-3, indicating activation of the apoptotic pathway (Fig. 9).

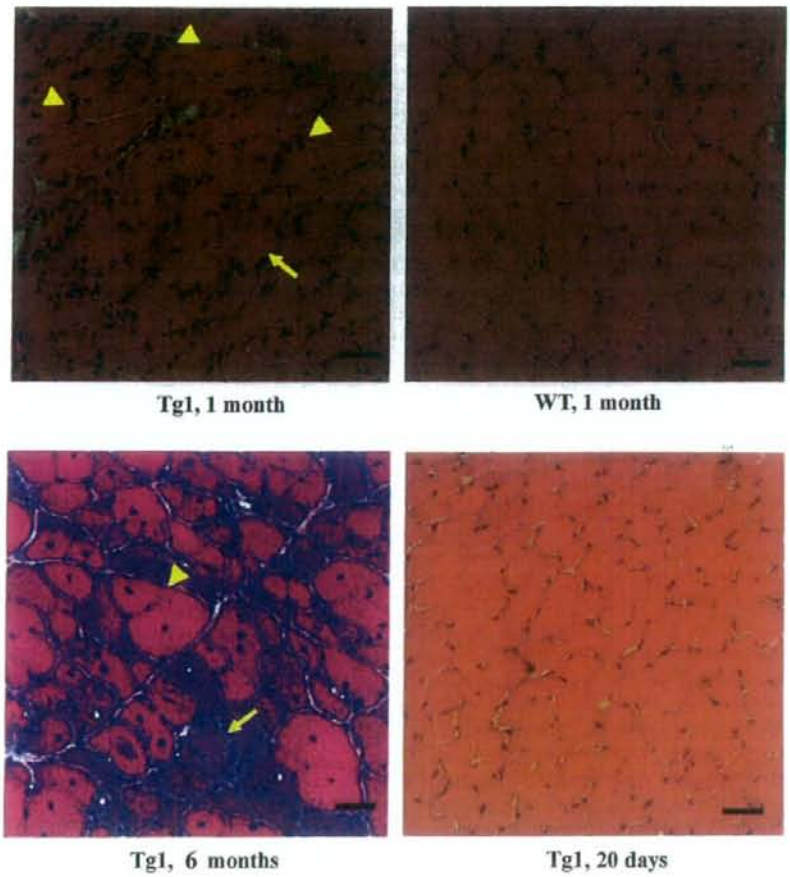

Fig. 4. Progressive myofiber degeneration of Tg1 mice. Hematoxylin and eosin staining of gastrocnemius muscles of Tg1 mice at the age of 20 days, 1 mo, and 6 mo. At the age of 1 mo, faintly stained degenerative myofibers (arrow) and centronucleated myofibers appeared in the Tg1 mouse, in contrast to the WT littermate. Arrowheads indicate the infiltration of mononuclear cells. At the age of 6 mo, centronucleated myofibers were more predominant, with prominent differences in size. Fiber splitting (arrowhead) is also indicated. No histological abnormalities were noted at the age of 20 days. Scale bars: 40 μm.

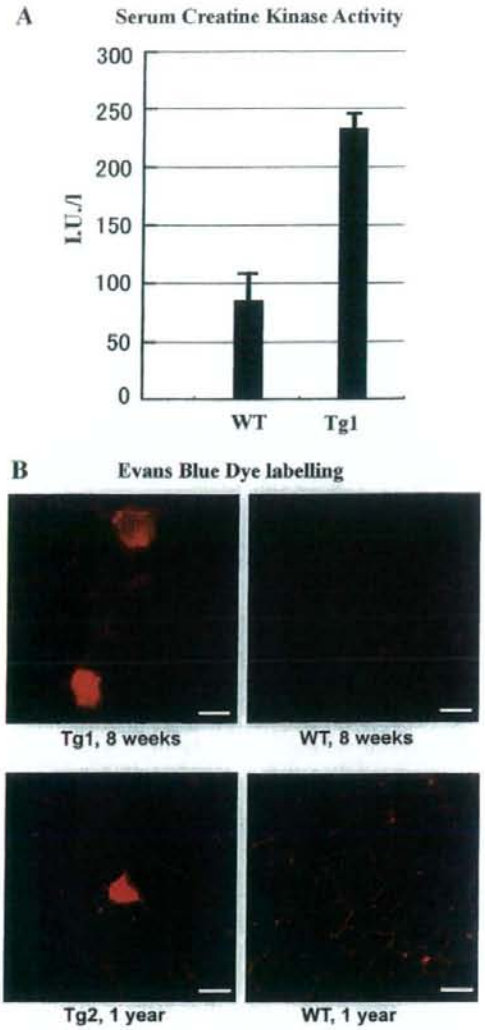

Fig. 5. Evaluation of membrane permeability of Tg1 skeletal muscle. *A*: serum creatine kinase (CK) activity of Tg1 mice at the age of 3 mo. Tg1 mice showed significantly higher CK activity than WT littermates ($P < 0.01$). *B*: after Evans blue dye injections, some myofibers of Tg1 mice and 1-yr-old Tg2 mice accumulated the dye in cytoplasm, showing increased membrane permeability. Scale bars: 40 μm.

Other pathological changes and food intake in the mBD-6 overexpressing mouse. mBD-6 overexpression decreases body weights and increases centronucleated myofibers and degenerative myofibers in mice. Kyphosis of vertebra, shortness in height, and slow movement were observed in the mouse. The food intake of Tg1 mice was significantly lower than that of the wild-type littermates. The short lifespan of Tg1 mice was evident, especially after they were backcrossed to the C57BL6/J strain. Many Tg1 mice died before 8 mo, and no mice backcrossed to the C57BL6/J strain lived for >1 yr. There was no evidence of cancer in the dead Tg1 mice.

DISCUSSION

Our data first demonstrated the pathogenic effects of dysregulated β-defensin expression in vivo. Western blot analysis of muscle extracts ascertained the overproduction of mature mBD-6 peptide in the Tg1 and Tg2 mice. The dysregulated β-defensin expression induced poor growth, short lifespan, and functional muscle impairment. Pathologically, the skeletal muscle of Tg1 mice showed progressive degeneration and regeneration of myofibers, consistent with the histology of muscular dystrophy. Elevated serum CK activity and positive Evans blue dye labeling in Tg1 mice indicated the disruption of the myofiber plasma membrane, also consistent with muscular dystrophy.

Despite recent identification of causative genes, the clinical course of muscular dystrophy is miserable lacking an established therapy. Although gene therapy could be curative, replacing the ultimate defect, many obstacles exist to technical progress. So, presently, important therapy targets are the factors modulating the state of muscle degeneration. Clinically,

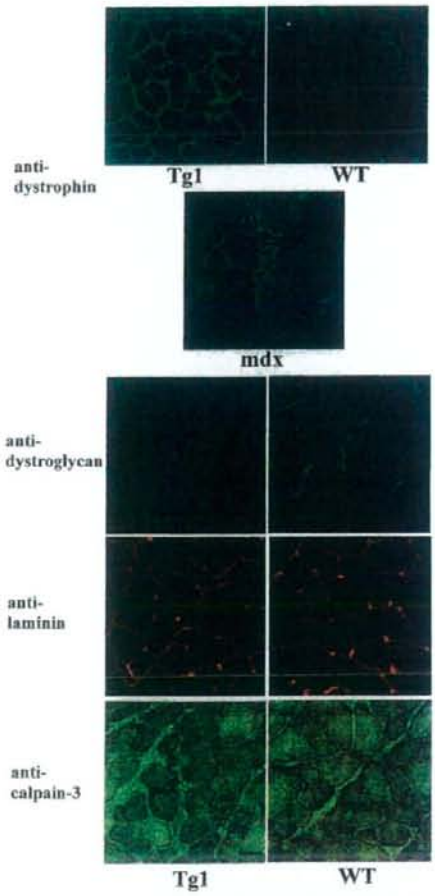

Fig. 6. Immunohistochemical analyses of dystrophin, α-dystroglycan, laminin, and calpain-3 distributions in Tg1 skeletal muscle. Distribution of these molecules in Tg1 mice showed no difference from WT. Dystrophin is absent in dystrophin-deficient muscle (mdx). Scale bars: 20 μm.

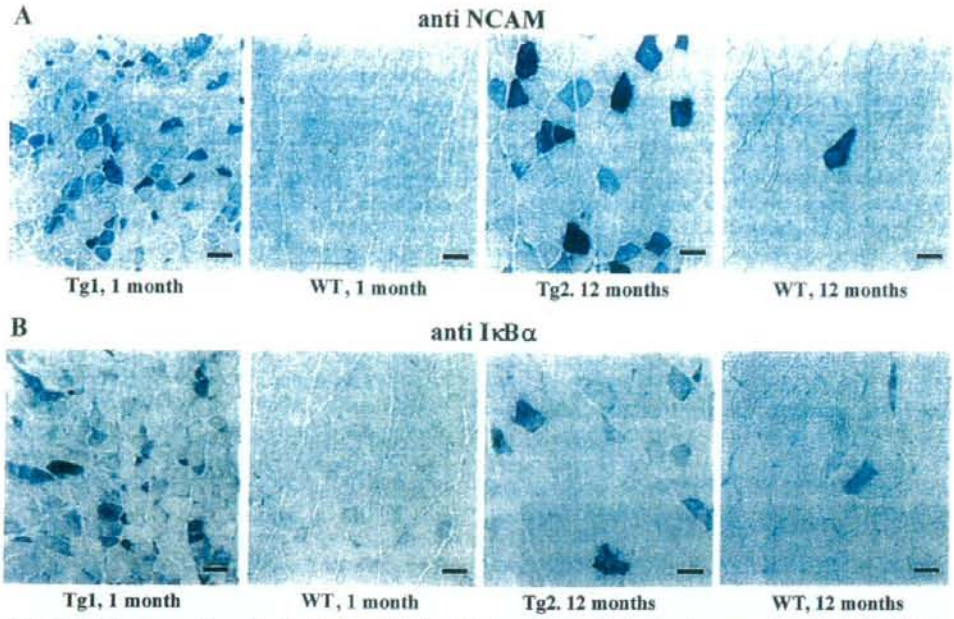

Fig. 7. Immunohistochemical analyses of neural cell adhesion molecule (NCAM) and IκBα distributions in young Tg1 mice and aged Tg2 mice. *A*: many myofibers showed a high level of expression of NCAM in 1-mo-old Tg1 mice and 12-mo-old Tg2 mice, in contrast to WT littermates. *B*: many myofibers showed accumulation of IκBα in 1-mo-old Tg1 mice and 12-mo-old Tg2 mice, in contrast to WT littermates. Scale bars: 40 μm.

glucocorticoids are utilized to delay the progression of Duchene muscular dystrophy (12, 20, 34), and, actually, the invasion of lymphoid and myeloid cells is an early stage feature of Duchene muscular dystrophy (33). β-Defensin would be the first reported component of inflammation that induced alone the typical phenotype of muscular dystrophy. Because mBD-6 and human defensin-3 showed intrinsic expression in skeletal muscle (10, 39), and invaded myeloid cells and lymphocytes would secrete abundant α-defensin in human muscular dystrophy (42), our findings suggest the significance of the defensin family in the pathogenesis of muscular dystrophy.

In aged Tg2 mice, mBD-6 overexpression induced NCAM-positive myofibers and IκBα accumulation with mild histological abnormality. Interestingly, aging alone induced a slight increase in NCAM-positive myofibers and IκBα-positive myofibers. The augmentation of these aging phenomena in Tg2 mice suggested that defensin-mediated muscle degeneration would not be limited to distinct muscular dystrophy but would

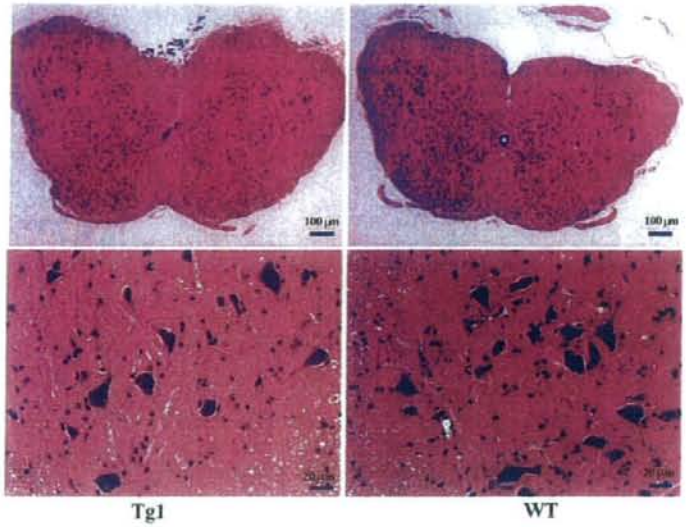

Fig. 8. Hematoxylin and eosin staining of spinal cords of Tg1 mouse and WT littermate. No. and morphology of motor neurons showed no abnormality causative of myofiber degeneration in the Tg1 mouse.

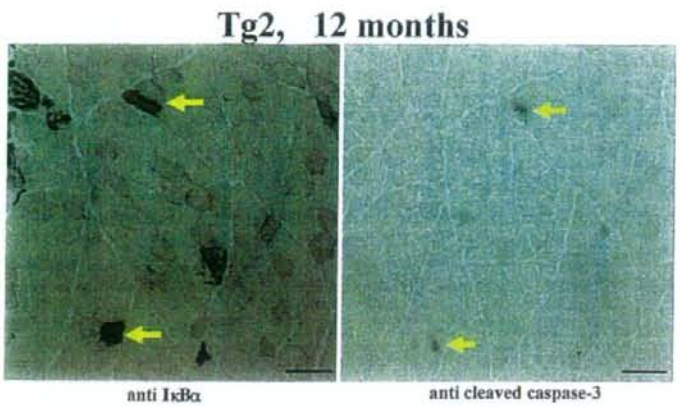

Fig. 9. Apoptotic feature of Tg2 skeletal muscle. Immunohistochemical analysis of serial sections for IκBα and cleaved caspase-3 indicated that some myofibers (arrow) showed both accumulation of IκBα and apoptotic features. Scale bars: 40 μm.

be associated with a much more common late-onset muscular wasting degeneration like sarcopenia, cachexia, or senescence acceleration.

Previous studies with transgenic mice overexpressing antimicrobial proteins (e.g., lysozyme) or peptides (e.g., human defensin-5) have indicated the beneficial roles of these substances in the in vivo situation (1, 27). In contrast to these animal models, Tg1 mice succumbed to muscular degeneration and short lifespan, showing a completely novel aspect of antimicrobial peptides. The various mediators, like reactive oxygen metabolites, complement cascades, and some proteases are involved in the known immune-mediated tissue injury in inflammatory conditions. Our investigation has established the defensin family as a novel effector of immune-mediated tissue injury.

The molecular mechanism of defensin-mediated tissue injury remains to be clarified. Generally, pore formation and permeabilization of target membranes are common mechanisms of defensin effects (9, 18, 19). Because dystrophin, dystroglycan, and laminin distributions were normal, mBD-6 would induce muscle degeneration independently of the dystrophin-glycoprotein complex.

Although upregulation of NCAM was shown in denervated myofibers, the histology of motor neurons of Tg1 mice showed no abnormality that could be causative for massive myofiber degeneration. So, these NCAM-positive myofibers would indicate the regenerative process and/or association of motor endplate degeneration in Tg1 and Tg2 mice, as indicated in some types of muscular dystrophy (7, 13, 38). At the same time, the accumulation of IκBα in Tg1 and Tg2 mice with apoptotic features is similar to that in LGMD2A patients and their animal models (2, 25). In LGMD2A patients, the defect of IκBα turnover inhibited the activity of NF-κB, associated with myofiber apoptosis. Because perturbation of the NF-κB/IκB pathway could cause the subsequent perturbation of many survival genes, it could be a common pathway in various mechanisms of myofiber degeneration.

The next question is, what downstream events of the β-defensin-6 pathway might be involved in the mechanisms of myofiber degeneration? Actually, both CCR6 and TLR4 are expressed in skeletal muscle. Other investigators (8) have reported that TLR4 expression is identified in skeletal muscles. We also confirmed the expression of TLR4 using RT-PCR. However, we do not think that the downstream events of the β-defensin-6 pathway are important in the pathogenesis of the muscle degeneration phenotype. Until now, there have been no data about the pathological relationship between muscle degeneration and TLRs. While various functions of the defensin family in mammalian cells have been reported, including cytotoxicity, most of the downstream events were not clarified, and the contribution of CCR6 or TLR4 on the pathogenesis of muscle degeneration would be limited, if it existed. Certainly, CCR6 receptors and TLR4 are expressed in skeletal muscle, and the NF-κB pathway is directly associated with TLR4. However, it is reasonable to speculate that continuous stimulation of these receptors does not primarily contribute to induce degeneration of myofibers in vivo. If such a phenomenon were to happen, the muscles could be totally abolished, and severe muscle damage would occur earlier in life.

In this study, body weights of Tg1 mice were significantly lower than for wild-type mice. Food intake of Tg1 mice was significantly lower than for wild-type littermates. The decreased food intake could explain, in part, decreased body weight. However, prominent myofiber degeneration could never be induced by decreased food intake, and it is more likely that decreased food intake resulted from decreased muscular mass and strength. Furthermore, Tg1 mice had a short life span. Most Tg1 mice died before 11 mo of age. The short lifespan of Tg1 mice was especially evident after they were backcrossed to the C57Bl6/J strain. Many Tg1 mice died before 8 mo, and no mice backcrossed to the C57BL6/J strain lived for >1 yr. We could not clarify the specific cause of Tg1 mouse death except severe loss of body weight. There was no evidence of cancer in the dead Tg1 mice; thus we speculate that impaired immune function may cause systemic inflammation and decreased food intake at a relatively young age, resulting in a malnutrition-related short lifespan.

In conclusion, our study has demonstrated that the defensin family could contribute to the pathogenic immune response in animal models, especially in the pathogenesis of myofiber degeneration.

ACKNOWLEDGMENTS

We thank H. Sugita and I. Nonaka for helpful discussion. We also thank H. Sorimachi for providing calpain-3 antibody and J. Miyazaki for the pCAGGS plasmid.

GRANTS

This work was supported in part by Grants-in-Aid for Scientific Research from the Ministry of Education, Science, Sports and Culture of Japan, Grants-in-Aid for Comprehensive Research on Aging and Health from the Ministry of Health, Labor and Welfare of Japan, and a Research Grant from Uehara Memorial Foundation.

REFERENCES

1. **Akinbi HT, Epaud R, Bhatt H, Weaver TE.** Bacterial killing is enhanced by expression of lysozyme in the lungs of transgenic mice. *J Immunol* 165: 5760–5766, 2000.
2. **Baghdiguian S, Martin M, Richard I, Pons F, Astier C, Bourg N, Hay RT, Chemaly R, Halaby G, Loiselet J, Anderson LV, Lopez de Munain A, Fardeau M, Mangeat P, Beckmann JS, Lefranc G.** Calpain 3 deficiency is associated with myonuclear apoptosis and profound perturbation of the IkappaB alpha/NF-kappaB pathway in limb-girdle muscular dystrophy type 2A. *Nat Med* 5: 503–511, 1999.
3. **Bals R, Wang X, Meegalla RL, Wattler S, Weiner DJ, Nehls MC, Wilson JM.** Mouse beta-defensin 3 is an inducible antimicrobial peptide expressed in the epithelia of multiple organs. *Infect Immun* 67: 3542–3547, 1999.
4. **Becker MN, Diamond G, Verghese MW, Randell SH.** CD14-dependent lipopolysaccharide-induced beta-defensin-2 expression in human tracheobronchial epithelium. *J Biol Chem* 275: 29731–29736, 2000.
5. **Biragyn A, Ruffini PA, Leifer CA, Klyushnenkova E, Shakhov A, Chertov O, Shirakawa AK, Farber JM, Segal DM, Oppenheim JJ, Kwak LW.** Toll-like receptor 4-dependent activation of dendritic cells by beta-defensin 2. *Science* 298: 1025–1029, 2002.
6. **Dalkilic I, Kunkel LM.** Muscular dystrophies: genes to pathogenesis. *Curr Opin Genet Dev* 13: 231–238, 2003.
7. **Deconinck AE, Rafael JA, Skinner JA, Brown SC, Potter SC, Metzinger L, Watt DJ, Dickson JG, Tinsley JM, Devies KE.** Utrophin-dystrophin-deficient mice as a model for Duchenne muscular dystrophy. *Cell* 90: 717–727, 1997.
8. **Frost RA, Nystrom GJ, Lang CH.** Lipopolysaccharide stimulates nitric oxide synthase-2 expression in murine skeletal muscle and C(2)C(12) myoblasts via Toll-like receptor-4 and c-Jun NH(2)-terminal kinase pathways. *Am J Physiol Cell Physiol* 287: C1605–C1615, 2004.
9. **Ganz T.** Defensins: antimicrobial peptides of innate immunity. *Nat Rev Immunol* 3: 710–720, 2003.
10. **Garcia JR, Jaumann F, Schulz S, Krause A, Rodriguez-Jimenez J, Forssmann U, Adermann K, Kluver E, Vogelmeier C, Becker D, Hedrich R, Forssmann WG, Bals R.** Identification of a novel, multifunctional beta-defensin (human beta-defensin 3) with specific antimicrobial activity. Its interaction with plasma membranes of Xenopus oocytes and the induction of macrophage chemoattraction. *Cell Tissue Res* 306: 257–264, 2001.
11. **Gera JF, Lichtenstein A.** Human neutrophil peptide defensins induce single strand DNA breaks in target cells. *Cell Immunol* 138: 108–120, 1991.
12. **Gosselin LE, McCormick KM.** Targeting the immune system to improve ventilatory function in muscular dystrophy. *Med Sci Sports Exerc* 36: 44–51, 2004.
13. **Grady RM, Akaaboune M, Cohen AL, Maimone MM, Lichtman JW, Sanes JR.** Tyrosine-phosphorylated and nonphosphorylated isoforms of alpha-dystrobrevin: roles in skeletal muscle and its neuromuscular and myotendinous junctions. *J Cell Biol* 160: 741–752, 2003.
14. **Harder J, Bartels J, Christophers E, Schröder JM.** A peptide antibiotic from human skin. *Nature* 387: 861, 1997.
15. **Harder J, Bartels J, Christophers E, Schröder JM.** Isolation and characterization of human beta-defensin-3, a novel human inducible peptide antibiotic. *J Biol Chem* 276: 5707–5713, 2001.
16. **Hoffmann JA, Kafatos FC, Janeway CA, Ezekowitz RA.** Phylogenetic perspectives in innate immunity. *Science* 284: 1313–1318, 1999.
17. **Laval SH, Bushby KM.** Limb-girdle muscular dystrophies–from genetics to molecular pathology. *Neuropathol Appl Neurobiol* 30: 91–105, 2004.
18. **Lehrer RI, Lichtenstein AK, Ganz T.** Defensins: antimicrobial and cytotoxic peptides of mammalian cells. *Annu Rev Immunol* 11: 105–128, 1993.
19. **Lichtenstein A.** Mechanism of mammalian cell lysis mediated by peptide defensins. Evidence for an initial alteration of the plasma membrane. *J Clin Invest* 88: 93–100, 1991.
20. **Mendell JR, Moxley RT, Griggs RC, Brooke MH, Fenichel GM, Miller JP, King W, Signore L, Pandya S, Florence J.** Randomized, double-blind six-month trial of prednisone in Duchenne's muscular dystrophy. *N Engl J Med* 320: 1592–1597, 1989.
21. **Nishimura M, Abiko Y, Kurashige Y, Takeshima M, Yamazaki M, Kusano K, Saitoh M, Nakashima K, Inoue T, Kaku T.** Effect of defensin peptides on eukaryotic cells: primary epithelial cells, fibroblasts and squamous cell carcinoma cell lines. *J Dermatol Sci* 36: 87–95, 2004.
22. **Niwa H, Yamamura K, Miyazaki J.** Efficient selection for high-expression transfectants with a novel eukaryotic vector. *Gene* 108: 193–200, 1991.
23. **Niyonsaba F, Ushio H, Nagaoka I, Okumura K, Ogawa H.** The human beta-defensins (-1, -2, -3, -4) and cathelicidin LL-37 induce IL-18 secretion through p38 and ERK MAPK activation in primary human keratinocytes. *J Immunol* 175: 1776–1784, 2005.
24. **Richard I, Broux O, Allamand V, Fougerousse F, Chiannilkulchai N, Bourg N, Brenguier L, Devaud C, Pasturaud P, Roudaut C, Hillaire D, Passos-Bueno MR, Zatz M, Tischfield JA, Fardeau M, Jackson CE, Cohen D, Beckmann JS.** Mutations in the proteolytic enzyme calpain 3 cause limb-girdle muscular dystrophy type 2A. *Cell* 7: 27–40, 1995.
25. **Richard I, Roudaut C, Marchand S, Baghdiguian S, Herasse M, Stockholm D, Ono Y, Suel L, Bourg N, Sorimachi H, Lefranc G, Fardeau M, Sebille A, Beckmann JS.** Loss of calpain 3 proteolytic activity leads to muscular dystrophy and to apoptosis-associated IkappaBalpha/nuclear factor kappaB pathway perturbation in mice. *J Cell Biol* 151: 1583–1590, 2000.
26. **Sakamoto N, Mukae H, Fujii T, Ishii H, Yoshioka S, Kakugawa T, Sugiyama K, Mizuta Y, Kadota J, Nakazato M, Kohno S.** Differential effects of alpha- and beta-defensin on cytokine production by cultured human bronchial epithelial cells. *Am J Physiol Lung Cell Mol Physiol* 288: L508–L513, 2005.
27. **Salzman NH, Ghosh D, Huttner KM, Paterson Y, Bevins CL.** Protection against enteric salmonellosis in transgenic mice expressing a human intestinal defensin. *Nature* 422: 522–526, 2003.
28. **Sawicki W, Mystkowska ET.** Contraceptive potential of peptide antibiotics. *Lancet* 353: 464–465, 1999.
29. **Schröder JM.** Epithelial antimicrobial peptides innate local host response elements. *Cell Mol Life Sci* 56: 32–46, 1999.
30. **Spence HJ, Chen YJ, Winder SJ.** Muscular dystrophies, the cytoskeleton and cell adhesion. *Bioessays* 24: 542–552, 2002.
31. **Spencer MJ, Guyon JR, Sorimachi H, Potts A, Richard I, Herasse M, Chamberlain J, Dalkilic I, Kunkel LM, Beckmann JS.** Stable expression of calpain 3 from a muscle transgene in vivo: immature muscle in transgenic mice suggests a role for calpain 3 in muscle maturation. *Proc Natl Acad Sci USA* 99: 8874–8879, 2002.
32. **Spencer LT, Paone G, Krein PM, Rouhani FN, Rivera-Nieves J, Brantly ML.** Role of human neutrophil peptides in lung inflammation associated with alpha1-antitrypsin deficiency. *Am J Physiol Lung Cell Mol Physiol* 286: L514–L520, 2004.
33. **Spencer MJ, Tidball JG.** Do immune cells promote the pathology of dystrophin-deficient myopathies? *Neuromuscul Disord* 11: 556–564, 2001.
34. **St-Pierre SJ, Chakkalakal JV, Kolodziejczyk SM, Knudson JC, Jasmin BJ, Megeney LA.** Glucocorticoid treatment alleviates dystrophic myofiber pathology by activation of the calcineurin/NF-AT pathway. *FASEB J* 18: 1937–1939, 2004.
35. **Tagawa K, Taya C, Hayashi Y, Nakagawa M, Ono Y, Fukuda R, Karasuyama H, Toyama-Sorimachi N, Katsui Y, Hata S, Ishiura S, Nonaka I, Seyama Y, Arahata K, Yonekawa H, Sorimachi H, Suzuki K.** Myopathy phenotype of transgenic mice expressing active site-mutated inactive p94 skeletal muscle-specific calpain, the gene product responsible for limb girdle muscular dystrophy type 2A. *Hum Mol Genet* 9: 1393–1402, 2000.
36. **Valore EV, Park CH, Quayle AJ, Wiles KR, McCray PB Jr, Ganz T.** Human beta-defensin-1: an antimicrobial peptide of urogenital tissues. *J Clin Invest* 101: 1633–1642, 1998.
37. **Van Wetering S, Sterk PJ, Rabe KF, Hiemstra PS.** Defensins: key players or bystanders in infection, injury, and repair in the lung? *J Allergy Clin Immunol* 104: 1131–1138, 1999.
38. **Winter A, Bornemann A.** NCAM, vimentin and neonatal myosin heavy chain expression in human muscle diseases. *Neuropathol Appl Neurobiol* 25: 417–424, 1999.
39. **Yamaguchi Y, Fukuhara S, Nagase T, Tomita T, Hitomi S, Kimura S, Kurihara H, Ouchi Y.** A novel mouse β-defensin, mBD-6, predomi-

nantly expressed in skeletal muscle. *J Biol Chem* 276: 31510–31514, 2001.

40. **Yang D, Biragyn A, Kwak LW, Oppenheim JJ.** Mammalian defensins in immunity: more than just microbicidal. *Trends Immunol* 23: 291–296, 2002.
41. **Yang D, Chertov O, Bykovskaia SN, Chen Q, Buffo MJ, Shogan J, Anderson M, Schröder JM, Wang JM, Howard OM, Oppenheim JJ.** Beta-defensins: linking innate and adaptive immunity through dendritic and T cell CCR6. *Science* 286: 525–528, 1999.
42. **Zhang L, Yu W, He T, Yu J, Caffrey RE, Dalmasso EA, Fu S, Pham T, Mei J, Ho JJ, Zhang W, Lopez P, Ho DD.** Contribution of human alpha-defensin 1, 2, and 3 to the anti-HIV-1 activity of CD8 antiviral factor. *Science* 298: 995–1000, 2002.

J Appl Physiol 102: 2361–2368, 2007.
First published March 1, 2007; doi:10.1152/japplphysiol.00615.2006.

Adrenomedullin insufficiency increases allergen-induced airway hyperresponsiveness in mice

Hiroshi Yamamoto,[1] Takahide Nagase,[2] Takayuki Shindo,[3] Shinji Teramoto,[1] Tomoko Aoki-Nagase,[1] Yasuhiro Yamaguchi,[1] Yoko Hanaoka,[1] Hiroki Kurihara,[4] and Yasuyoshi Ouchi[1]

Departments of [1]Geriatric Medicine, [2]Respiratory Medicine, and [4]Physiological Chemistry and Metabolism, Graduate School of Medicine, University of Tokyo, Tokyo; and [3]Department of Organ Regeneration, Shinshu University Graduate School of Medicine, Nagano, Japan

Submitted 2 June 2006; accepted in final form 25 February 2007

Yamamoto H, Nagase T, Shindo T, Teramoto S, Aoki-Nagase T, Yamaguchi Y, Hanaoka Y, Kurihara H, Ouchi Y. Adrenomedullin insufficiency increases allergen-induced airway hyperresponsiveness in mice. *J Appl Physiol* 102: 2361–2368, 2007. First published March 1, 2007; doi:10.1152/japplphysiol.00615.2006.—Adrenomedullin (ADM), a newly identified vasodilating peptide, is reported to be expressed in lungs and have a bronchodilating effect. We hypothesized whether ADM could be involved in the pathogenesis of bronchial asthma. We examined the role of ADM in airway responsiveness using heterozygous ADM-deficient mice ($AM^{+/-}$) and their littermate control ($AM^{+/+}$). Here, we show that airway responsiveness is enhanced in ADM mutant mice after sensitization and challenge with ovalbumin (OVA). The immunoreactive ADM level in the lung tissue after methacholine challenge was significantly greater in the wild-type mice than that in the mutant. However, the impairment of ADM gene function did not affect immunoglobulins (OVA-specific IgE and IgG1), T helper 1 and 2 cytokines, and leukotrenes. Thus the conventional mechanism of allergen-induced airway responsiveness is not relevant to this model. Furthermore, morphometric analysis revealed that eosinophilia and airway hypersecretion were similarly found in both the OVA-treated ADM mutant mice and the OVA-treated wild-type mice. On the other hand, the area of the airway smooth muscle layer of the OVA-treated mutant mice was significantly greater than that of the OVA-treated wild-type mice. These results suggest that ADM gene disruption may be associated with airway smooth muscle hyperplasia as well as enhanced airway hyperresponsiveness. ADM mutant mice might provide novel insights to study the pathophysiological role of ADM in vivo.

asthma; airway hyperresponsiveness; remodeling; adrenomedullin; knockout mouse

ADRENOMEDULLIN (ADM) is a newly identified vasodilating peptide initially isolated from the extracts of human pheochromocytoma tissue (14). This peptide, which consists of 52 amino acids in human, belongs to the CGRP/CT superfamily of peptides including calcitonin (CT), amylin, and CT gene-related peptide (CGRP). ADM mRNA is demonstrated in a number of tissues, abundant in adrenal medulla, atrium, and lung (7), whereas ADM also circulates in the plasma (13). McLatchie et al. demonstrated that the CT-receptor-like receptor functions as an ADM receptor in the presence of receptor-activity-modifying protein 2 (17). They also demonstrated that the expression of receptor-activity-modifying protein 2 component was strongly recognized in the lung. Although it is speculated that ADM plays an important role in the lung tissue, the exact roles of ADM gene function on airway inflammation and airway remodeling remain little known.

In animals, Kanazawa and colleagues have reported that ADM inhibits histamine- or acetylcholine-induced bronchoconstriction in anesthetized guinea pigs (12) and that its bronchodilating effect is as potent as isoproterenol. They also demonstrated that the precursor of ADM, i.e., proadrenomedullin NH_2-terminal 20 peptide, has the same properties to induce bronchodilation (11). Furthermore, it has been demonstrated that ADM has the inhibitory effect on antigen-induced microvascular leakage and bronchoconstriction in guinea pigs (20). In humans, it was also reported that human plasma ADM levels correlated negatively with the degree of airway obstruction, as indicated by forced expiratory volume in 1 s; the plasma ADM concentration was associated with the severity of human asthma. This suggests that the level of ADM excretion may affect the degree of asthma severity or that asthma-related bronchoconstriction and/or hypoxia increases the ADM levels as a compensative mechanism (3). Thus it is reasonably assumed that ADM, proadrenomedullin NH_2-terminal 20 peptide, or their derivatives could be the new-generation bronchodilators used in the clinical settings. Meanwhile, the biological roles of innate ADM peptides based on ADM gene function in vivo remain unclear.

Because the familial or the genetic background is potentially associated with the etiology of asthma, a number of genes have been explored for the association of asthma (4). However, the exact molecular mechanisms underlying bronchial asthma still remain to be elucidated. We therefore hypothesized whether ADM gene could be involved in the pathogenesis of asthma.

Since the airway hyperresponsiveness (AHR) and inflammation including eosinophil infiltration are major characteristics of asthma (5, 6, 16), we examined the role of ADM in airway responsiveness using murine model of asthma. Although we recognized that homozygous ADM-deficient mice ($AM^{-/-}$) are best suitable for the current experiments, they are unfortunately embryonic lethal (23). We therefore performed the following experiments using heterozygous ADM-deficient mice ($AM^{+/-}$) and their littermate wild-type control ($AM^{+/+}$).

Then, we examined the relationship between the AHR and the lung inflammation including eosinophil infiltration and other inflammatory mediators in mutant mice and control mice. In murine lung model of allergen-induced hyperresponsive-

Address for reprint requests and other correspondence: H. Yamamoto, Dept. of Geriatric Medicine, Graduate School of Medicine, Univ. of Tokyo, 7-3-1 Hongo, Bunkyo-ku, Tokyo, Japan 113-8655 (e-mail: hyamamot-tky@umin.ac.jp).

The costs of publication of this article were defrayed in part by the payment of page charges. The article must therefore be hereby marked "*advertisement*" in accordance with 18 U.S.C. Section 1734 solely to indicate this fact.

ness, OVA challenge induces an eosinophilic inflammation, bronchial hyperresponsiveness, and production of specific IgE (15). However, the precise role of various types of inflammatory cells and mediators involved in the pathophysiology of AHR remains to be fully determined. Thus we further examined the other inflammatory mediators including immunoglobulins (OVA-specific IgE and IgG1), T helper (Th) 1 and Th2 cytokines, and leukotrienes (LTs).

In addition, the association of morphological changes with AHR in the murine model was examined. Because ADM is known to have anti-proliferative effect on smooth muscle cells and fibroblasts, altered ADM function may affect cell kinetics on airway wall, which may contribute to induction of AHR in the mice.

MATERIALS AND METHODS

Animals. Heterozygous ADM-deficient mice ($AM^{+/-}$) were established as previously described (23). Briefly, a targeting vector was constructed to replace the 2.4-kb fragment encompassing the 1.3-kb 5′-flanking region, exons 1–3, and part of exon 4 of proadrenomedullin with the neomycin resistance gene. The plasmid was linearized and then introduced into 129/Sv-derived SM-1 embryonic stem cells by electroporation. Homologous recombinants were identified by Southern blot analysis, and two independently targeted clones were injected into C57/BL6 blastocysts to generate chimeric mice. Male Chimeras were crossbred with C57/BL6 females, and germ-line transmission was verified by Southern blot analysis. All experiments were approved by the University of Tokyo Ethics Committee for Animal Experiments. For genotyping, genomic DNAs were isolated from biopsied tail and subjected to PCR amplification. The animals were maintained on a light-dark cycle with light from 0700 to 2000 at 23°C. Mice were fed with a standard laboratory diet and water ad libitum. Mutant mice and their littermate controls ($AM^{+/+}$), between 4 and 12 wk of age, were used in the current study. There was no difference in the body weight between the wild-type group and the mutant one [$AM^{+/+}$ saline (n = 11), 30.18 ± 0.76 g; $AM^{+/-}$ saline (n = 11), 30.36 ± 0.82 g; $AM^{+/+}$ OVA (n = 14), 29.00 ± 1.28 g; $AM^{+/-}$ OVA (n = 14), 29.79 ± 0.79 g].

Sensitization and antigen challenge. To develop allergen-induced asthma model mice, we performed allergen sensitization and inhalational antigen challenge as previously described (2). Briefly, on *day 1*, $AM^{+/+}$ or $AM^{+/-}$ mice were randomly selected and sensitized with intraperitoneal (ip) injection of 0.5 ml solution containing 0.1 mg OVA mixed with aluminum hydroxide (2 mg/ml). On *day 8*, the mice were subsequently boosted with the same mixture. On *days 13* and *14*, these sensitized mice were placed in an 18 × 11 × 11 cm plastic chamber and were challenged for 60 min with aerosolized 1% OVA dissolved in saline, generated with an ultrasonic nebulizer (NE-U17, Omron). Others received ip injection of saline and saline aerosols in the same manner. On *day 15*, we performed measurement of bronchial responsiveness or bronchoalveolar lavage (BAL).

Animal preparation. Animals were anesthetized with pentobarbital sodium (25 mg/kg ip) and ketamine hydrochloride (25 mg/kg ip) in combination and then paralyzed with pancuronium bromide (0.3 mg/kg ip). After tracheostomy, an endotracheal metal tube (inside diameter of 1 mm, length of 8 mm) was inserted in the trachea. Animals were mechanically ventilated (model 683, Harvard Apparatus, South Natick, MA) with tidal volumes of 10 ml/kg and frequencies of 2.5 Hz. An incision was made on the abdominal wall, then the diaphragm of the bilateral chest was incised and the chest was widely opened. Positive end-expiratory pressure of 2 cmH_2O was applied by placing the expired line underwater. During the experiments, oxygen gas was continuously supplied to the ventilatory system. A heating pad was used to maintain the body temperature of animals. Tracheal pressure was measured with a piezoresistive micro transducer (Endevco 8510B-2, San Juan Capistrano) placed in the lateral port of the tracheal cannula. Tracheal flow was measured by means of a Fleisch pneumotachograph (model no. 00000, Metabo SA, Lausanne, Switzerland). All signals were amplified, filtered at a cutoff frequency of 100 Hz, and converted from analog to digital with a converter (DT2801-A, Data Translation, Marlborough, MA). The signals were sampled at a rate of 200 Hz and stored on an IBM-AT compatible computer. Lung resistance (R_L) and elastance were measured as previously described (19).

Airway responsiveness to methacholine administration. At the start of the protocol, two deep inhalations (3 times tidal volume) were delivered to standardize volume history. All animals were then challenged with saline aerosol for 2 min. Aerosols were generated by an ultrasonic nebulizer (Ultra-Neb100, DeVilbiss, Somerset, PA) and delivered through the inspiratory line into the trachea. Measurements of 10-s duration were sampled during tidal ventilation 1 min after administration of saline aerosol. This represented the baseline measurement. Then, each dose of methacholine (MCh) aerosol was administered for 2 min, and measurements were performed 1 min after each MCh inhalation in a dose-response manner (0.3125, 0.625, 1.25, 2.5, 5, 10, 20, 40, and 80 mg/ml). Airway responsiveness was assessed using the concentration of MCh required to increase R_L to 200% of baseline values ($EC_{200}R_L$) (18).

BAL fluid. BAL was performed using 1 ml of PBS 5 times in each group. In each animal, ~90% (4.5 ml) of the total injected volume was consistently recovered. After BAL fluid (BALF) was centrifuged at 450 *g* for 10 min, the total and differential cell counts of the BALF were determined from the cell fraction. The supernatant was stored at −80°C until assays were performed. The concentration of protein was measured by Bradford's method using bovine serum albumin as a standard.

Assay of total immunoglobulin E (IgE) in BALF. Total amount of IgE was assayed followed by the PharMingen protocol (http://www.bdbiosciences.com/pharmingen/protocols/Mouse_IgE_ELISA.shtml). The purified anti-mouse IgE capture monoclonal antibody (BD PharMingen, catalog no. 02111D, clone R35-72) was used for the assay. The antibody titers were calculated by comparison with standard samples using serum of an OVA-immunized mouse and analyzed with the Microplate Manager software for the Macintosh computer (Bio-Rad). The detection limit of the ELISA assays for IgE was 4.59 ng/ml.

Assay of OVA-specific IgE in serum. OVA-specific IgE was assayed in a manner similar to the PharMingen protocol of IgE. Briefly, 96-well flat-bottomed ELISA plates were coated with the purified anti-mouse IgE capture monoclonal antibody (BD PharMingen, catalog no. 553413, clone R35-72) and conjugated with biotinylated OVA and SAv-HRP. We measured the absorbance on the microplate

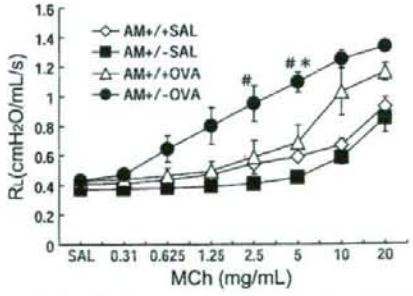

Fig. 1. Methacholine (MCh) dose response curves for lung resistance (R_L) in the wild-type and the heterozygous adrenomedullin (ADM) mutant mice. SAL, saline; OVA, ovalbumin. *$P < 0.05$ compared with the R_L in the same MCh dosage of $AM^{+/+}$ OVA group. #$P < 0.05$ compared with the R_L in the same MCh dosage of $AM^{+/-}$ SAL group.

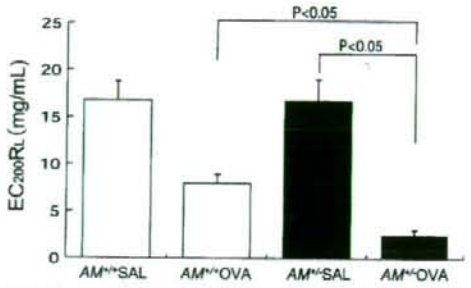

Fig. 2. $EC_{200}R_L$, Concentration of MCh required to increase R_L to 200% of baseline values. *$P < 0.05$ compared with the value of $AM^{+/+}$ OVA group. #$P < 0.05$ compared with the value of $AM^{+/-}$ SAL group.

reader set at 450 nm. The detection limit of the ELISA assays for OVA-specific IgE was 20 U/ml.

Assay of OVA-specific IgG1 in serum. An enhanced protein-binding ELISA plate was coated with the purified OVA. The plate was then blocked with 200 μl of blocking buffer per well. Samples or standards were put in each well at various dilutions in blocking buffer. Horseradish peroxidase-conjugated anti-mouse IgG1 (BD PharMingen, catalog no. 559626, clone X56) was diluted to 2 μg/ml in blocking buffer and was added respectively. The plate was incubated at room temperature for 30 min. Substrate buffer was added to develop color reaction at room temperature for 20–30 min. We measured the absorbance on the microplate reader set at 450 nm. The antibody titers were calculated by comparison with standard samples using serum of an OVA-immunized mouse and analyzed with the Microplate Manager software for the Macintosh computer (Bio-Rad). The detection limit of the ELISA assays for IgG1 was 142 U/ml.

Assays of LTs, IL-4, -5, and -13, and IFN-γ in BALF. LTC4/D4/E4 was measured using enzyme immunoassay kit (GE Healthcare Bio-Sciences, catalog no. RPN 224). Detection limit of LTC4/D4/E4 was 10 pg/ml. IL-4 and -5 and IFN-γ in BALF were measured using ELISA kits [Pierce Biotechnology, catalog no. EMIL42 (IL-4), EMIL52 (IL-5), EM1001 (IFN-γ)]. IL-13 in BALF was measured using mouse IL-13 immunoassay kit (Genzyme TECHNE, catalog no. 10003). Detection limits of the ELISA assays for IL-4, IL-5, IL-13, and IFN-γ were 15, 20, 7.8, and 37 pg/ml, respectively.

Assay of tissue ADM. Using lung specimens before and after MCh challenge, immunoreactive ADM (ir-ADM) levels in the lung tissues were measured using ADM[1–50](Mouse) RIA kit (Phoenix Pharmaceuticals, catalog no. RK-010-31). Before the assay, tissue sections were soaked in the 1.0 ml of 0.1 M acetic acid solution and were bathed in the 100°C water bath for 10 min. Then they were cooled down with ice, homogenized, and centrifuged at 13,000 *g* for 5 min at 4°C. The supernatant was used for the assay. The values of the ir-ADM were expressed as the quantity per gram wet tissue samples.

Semi-quantitative assessment of eosinophilia and airway mucus hypersecretion. Whole samples of tissue were fixed in 10% phosphate-buffered formalin (pH 7.4), embedded in paraffin, and cut into 4-μm sections. The sections were stained with hematoxylin and eosin, Luna, or periodic acid Schiff (PAS) and Alcian Blue co-staining. Each slide was provided for the count of cells. Eosinophil infiltration of the peribronchial tissue was estimated by using Luna stained slides. Goblet cell hyperplasia and airway mucus hypersecretion were assessed by inspecting PAS and Alcian blue stained slides. All slides were observed by the two uncensored persons and assessed by their subjective scoring from 0 (none) to 3 (abundant) under the microscope (Nikon). In terms of the reproducibility of this assessment, inter- or intraobserver variances were <5%.

Morphometric analysis of airway walls. Each section was also stained with Masson's trichrome for morphometric analysis and observed by systemic manner. The whole slide was scanned thoroughly and membranous bronchioles were carefully selected for the analysis. All selected regions are digitally photographed by the Nikon microscope. Measurements were performed by Image J software (version 1.37v, National Institutes of Health), using an IBM-compatible computer equipped with a digitizing tablet. Measurements are as follows: *1*) Abm means the area surrounded by the airway basement membrane, whose perimeter is Pbm; *2*) Amo means the area surrounded by the airway smooth muscle outline, whose perimeter is Psm; *3*) Ai means the internal airway lumen area, whose perimeter is Pi; *4*) the area of epithelial cells (Ae) is calculated by Abm − Ai, the area of smooth muscles (Asm) is also calculated by Amo − Abm; *5*) airway longer diameter is D_L, shorter one is Ds. Airway size was standardized by comparing Abm, i.e., Ai/Abm or Ae/Abm or Asm/Abm. Seventy-eight of 144 selected airway sections appeared in the slides were excluded by the following criteria: the short-to-long luminal diameter ratio (D_S/D_L) was under 0.6 or the borders ill-defined. When we deal with the smooth muscle bundles, we carefully outlined the edge of the smooth muscle layer, and if we encountered the interruption of the locus, we followed it smoothly to the basement membrane to maximally exclude extracellular matrix. If the interruption was longer than 10% of Pbm, we discarded the sections like this. All the other components were applied for the analysis. In the same way, analysis was performed for immunohistochemically stained sections.

We assessed the number of cells in the airway smooth muscle layer by counting the number of nuclei in the layer. To standardize by airway size, the nuclear cell count (NCC) was divided by Pbm^2; i.e., NCC/Pbm^2. The standardized number of nuclear cells in the airway smooth muscle layer was compared among four groups, i.e., saline-treated wild-type, saline-treated ADM mutant, OVA-treated wild-type, OVA-treated ADM mutant mice.

Immunohistochemical staining for alpha-smooth muscle actin. Immunohistochemistry was performed using monoclonal antibodies against alpha-smooth muscle actin (α-SM actin) (DAKO Cytomation, code M0851, clone 1A4). After tissue sections were deparafinized and rehydrated, antigen retrieval was accomplished by 15-min incubation at 121°C in 0.01 M citrate buffered solution (pH 6.0). Endogenous peroxidase activity was blocked by incubation in methanol containing 3% H_2O_2. Anti-α-SM actin antibody of 1:50 dilution was prepared together with ENVISION+/horseradish peroxidase kit for Mouse (DAKO Cytomation, catalog no. K4000), then incubated with normal mouse serum for 60 min. This conjugate was added on each section and visualized by DAB. Labeling controls were performed under the

Table 1. *Total cell counts and cell fractions in BALF in each experimental group*

	TCC (×10⁴)	Mφ, %	Lym, %	Eos, %	PMN, %
$AM^{+/+}$ saline ($n = 5$)	4.94±1.91	96.02±2.82	4.32±2.67	0.02±0.00	0.26±0.21
$AM^{+/-}$ saline ($n = 5$)	4.82±0.54	91.96±2.51	7.24±2.25	0.10±0.00	0.82±0.48
$AM^{+/+}$ OVA ($n = 5$)	40.20±18.22†	70.58±15.00	2.84±1.87	25.88±14.88*	0.72±0.45
$AM^{+/-}$ OVA ($n = 6$)	21.13±8.75	60.02±12.41†	4.00±1.60	35.30±12.84†	0.70±0.28

Values are means ± SE. TCC, total cell count; Mφ, macrophages; Lym, lymphocytes; Eos, eosinophils; PMN, polymorphonuclear cells; BALF, broncho alveolor lavage fluid. †$P < 0.05$ compared with the saline group in the same strain of animals. *$P < 0.01$ compared with the saline group in the same strain of animals.

Table 2. *Biochemical analysis of BALF*

	TP, μg/ml	IgE, ng/ml	IL-4, pg/ml	IL-5, pg/ml	IFN-γ, pg/ml	LT C4/D4/E4, pg/ml
$AM^{+/+}$ Saline (n = 5)	4.94±1.91	5.30±0.85	1,092.3±17.1	17.0±3.8	1,492.4±129.0	25.3±1.3
$AM^{+/-}$ Saline (n = 5)	4.82±0.54	4.44±0.92	834.1±28.2	10.2±1.2	1,548.4±119.2	4.3±0.5
$AM^{+/+}$ OVA (n = 9)	40.20±18.22	70.58±15.00	938.9±28.7	41.8±14.6	1,353.0±66.6	41.4±26.4
$AM^{+/-}$ OVA (n = 7)	21.13±8.75	60.02±12.41	759.3±23.0	23.9±7.1	1,624.3±119.2	15.6±4.8

Values are means ± SE. TP, total protein; IgE, immunoglobulin E; IL-4, interleukin-4; IL-5, interleukin-5; IFN-γ, interferon-γ; LT C4/D4/E4, leukotriene C4/D4/E4.

same conditions other than the usage of mouse IgG2a negative control (DAKO Cytomation, catalog no. X0943) instead of anti-α-SM actin antibody at the same immunoglobulin concentration.

Materials and chemicals. Materials and chemicals were obtained from Sigma Chemical (St. Louis, MO) unless otherwise specified.

Data analysis. Comparisons of data among the experimental groups were carried out with one-way ANOVA (Scheffe's test) or the nonparametric Kruskal-Wallis test. Statistical significance was determined by P values under 0.05, and errors are given in SE (standard error) unless otherwise stated. The program Microsoft Excel 2003 was used for data management, and all statistics were performed using SPSS II (SPSS Japan, version 14.0).

RESULTS

Airway responsiveness to MCh administration. There were no significant differences in baseline R_L and lung elastance among each group. MCh dose response curves for R_L are demonstrated in Fig. 1. $AM^{+/-}$ mice showed the elevation of R_L to MCh dose of 2.5–5 mg/ml, whereas the other groups exhibited no significant responses.

Airway responsiveness was also assessed using $EC_{200}R_L$ (Fig. 2: saline-treated $AM^{+/+}$, 16.81 ± 2.01 mg/ml; saline-treated $AM^{+/-}$, 16.73 ± 2.34 mg/ml; OVA-treated $AM^{+/+}$, 7.95 ± 0.98* mg/ml; OVA-treated $AM^{+/-}$, 2.41 ± 0.63 mg/ml, respectively; $^*P < 0.05$ vs. the other groups). Although bronchial hyperresponsiveness to MCh was observed in the OVA-challenged wild-type mice, responses in the OVA-challenged $AM^{+/-}$ mice were significantly enhanced compared with the OVA-treated wild-type mice.

Assessment of the BALF. Cell fractions in BALF are shown in Table 1, indicating the increases in the eosinophil fractions in the OVA-sensitized groups. No differences in the fraction and the number of BALF eosinophil were observed between the OVA-treated wild-type and the mutant mice. Measurements of total IgE levels [saline-treated $AM^{+/+}$, 5.30 ± 0.85 ng/ml (n = 5); saline-treated $AM^{+/-}$, 4.44 ± 0.92 ng/ml (n = 5); OVA-treated $AM^{+/+}$, 4.19 ± 2.33 ng/ml (n = 9); OVA-treated $AM^{+/-}$, 4.40 ± 1.69 ng/ml (n = 7), respectively] showed no significant differences among each group. Total protein amount in BALF was also assessed [saline-treated $AM^{+/+}$, 45.05 ± 12.40 μg/ml (n = 6); saline-treated $AM^{+/-}$, 43.35 ± 7.00 μg/ml (n = 5); OVA-treated $AM^{+/+}$, 82.47 ± 23.60 μg/ml (n = 9); OVA-treated $AM^{+/-}$, 69.64 ± 14.70 μg/ml (n = 7), respectively], but no differences were found among each group. IL-4, 5, IL-13, and IFN-γ were measured, but no difference was found between OVA-treated mutant mice and OVA-treated wild-type mice. The level of LTC4/D4/E4 in BALF obtained from each group was also measured, but no differences were found either (Table 2).

Table 3. *Immunoreactivity analysis of serum*

	OVA-specific IgG1, U/ml	OVA-Specific IgE, U/ml
$AM^{+/+}$ Saline	ND	ND
$AM^{+/-}$ Saline	ND	ND
$AM^{+/+}$ OVA (n = 6)	5,578.4±4,513.1	ND
$AM^{+/-}$ OVA (n = 7)	1,879.6±1,389.3	ND

Values are means ± SE. ND, not detected.

Assessment of the serum. Antigen exposure increased the OVA-specific IgG1 levels [OVA-treated wild-type mice, 5,578.40 ± 4,513.11 U/ml (n = 7); OVA-treated mutant mice, 1,879.62 ± 1,389.27 U/ml (n = 7); saline groups not detectable], whereas no difference was observed between OVA-treated mutant mice and OVA-treated wild-type mice. Meanwhile, the OVA-specific IgE in serum was not detectable (Table 3).

ir-ADM. ir-ADM levels in the lung tissue were demonstrated in Fig. 3. ir-ADM levels of OVA-treated groups did not significantly differ from those of OVA-untreated groups. ir-ADM levels of the mutant groups before MCh challenge were also lower than those of the wild-type groups. MCh inhalation enhanced these immunoreactivities of each group ($P < 0.01$). ir-ADM levels after MCh inhalation were significantly different between OVA-untreated wild-type mice and OVA-untreated mutant mice ($P < 0.01$). Similarly, ir-ADM level of the OVA-treated mutant mice after MCh challenge was lower than that of the OVA-treated wild-type mice ($P < 0.01$).

Semi-quantitative assessment of eosinophilia and airway hypersecretion. As shown in Fig. 4, mononuclear cells or eosinophils infiltrated markedly along the airways of the OVA-treated mice, whereas no difference was found between the wild-type and the mutant mice. On the Luna-stained tissue, eosinophils were markedly found around the airways of the OVA-challenged groups, but the degree of eosinofil infiltration showed no significant difference between the $AM^{+/+}$ and the

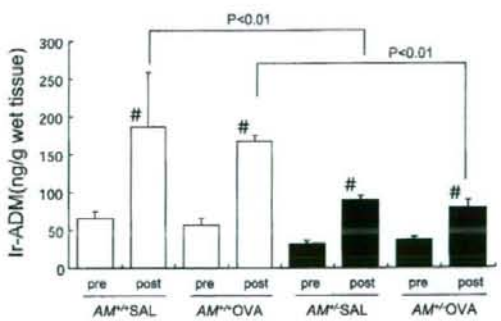

Fig. 3. Immunoreactive (Ir-) ADM in the lung before and after MCh challenge (RIA). $P < 0.01$ compared with the postinhalation value of $AM^{+/+}$ OVA group. #$P < 0.01$ compared with the preinhalation value.

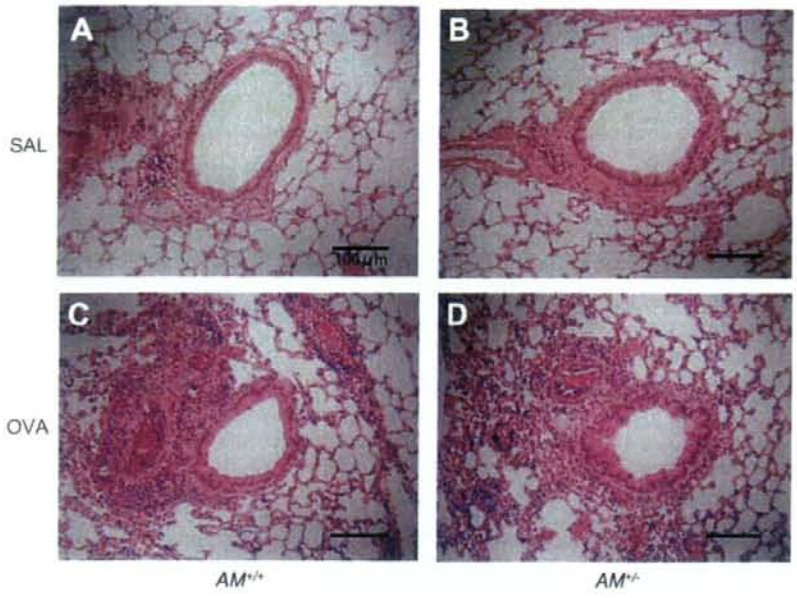

Fig. 4. Photomicrographs of small airways and lung parenchyma from saline-treated wild-type (*A*), saline-treated ADM mutant (*B*), OVA-treated wild-type (*C*), or OVA-treated ADM mutant mice (*D*). Specimens were stained with hematoxylin and eosin. Scale bar, 100 μm.

$AM^{+/-}$ mice (Fig. 5). OVA-treated groups apparently showed very intense staining of PAS/Alcian blue, suggesting goblet cell hyperplasia and airway mucus hypersecretion. Although the OVA challenge caused the significant change in both animal groups, the magnitude of goblet cell hyperplasia and airway mucus hypersecretion was not different between the wild-type mice and the mutant mice (Fig. 6).

Morphometric analysis. Ai/Abm of the OVA-treated mutant mice was significantly smaller than that of the OVA-untreated mutant type mice ($P = 0.0007$), but it was not different from that of the OVA-treated wild-type mice ($P = 0.20$) (Fig. 7). Ae/Abm of the OVA-treated mutant mice was greater than that of the OVA-untreated mutant mice ($P = 0.00007$), but it was not different from that of the OVA-treated wild-type mice ($P = 0.20$) (Fig. 8). Similarly, Asm/Abm of the OVA-treated mutant mice was also larger than that of the OVA-untreated mutant mice ($P = 0.00007$). However, Asm/Abm of the OVA-treated mutant mice was significantly greater than that of the OVA-treated wild-type mice ($P = 0.00010$) (Fig. 9). The number of cells in the airway smooth muscle layer of the OVA-treated mutant mice was significantly greater than that of the OVA-untreated mutant mice ($P = 0.0019$) or that of the OVA-treated wild-type mice ($P = 0.012$) (Fig. 10).

Assessment of airway smooth muscle mass of the tissue sections immunohistochemically stained with α-SM actin antibody (Fig. 11) was also performed. Asm/Abm of the OVA-treated mutant mice was significantly greater than that of the OVA-treated wild-type mice ($P = 0.0004$) (Fig. 12).

DISCUSSION

The current study clearly revealed greater AHR of the heterozygous ADM mutant mice in the allergen-induced asthma model. To our knowledge, this is the first report to study whether ADM gene function could be involved in the AHR using mutant mice. In addition, the MCh dose, which causes significant elevation of R_L in $AM^{+/-}$ mice, was very lower than that of the usual model of AHR in other mice. Thus the enhanced AHR suggests that innate ADM might play a pivotal role in AHR in allergen-induced asthma.

We observed that ir-ADM level after MCh challenge was significantly greater in the wild than in the mutant. This finding

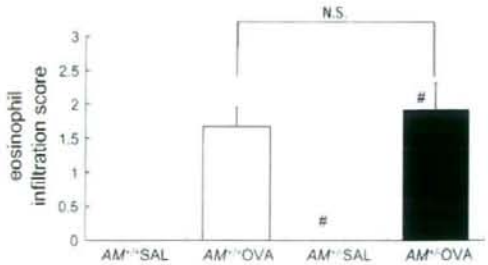

Fig. 5. Semi-qantitative assessment of eosinophil infiltration around the airways. #$P < 0.05$ compared with the saline group in the same strain.

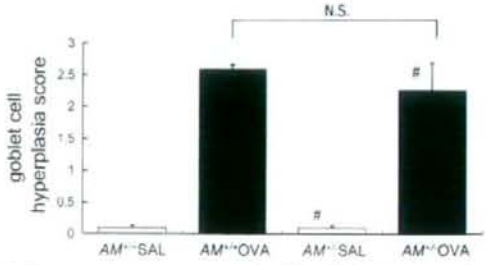

Fig. 6. Semi-quantitative assessment of goblet cell hyperplasia and airway hypersecretion of wild-type and mutant mice with OVA inhalation challenge. #$P < 0.05$ compared with the saline group.

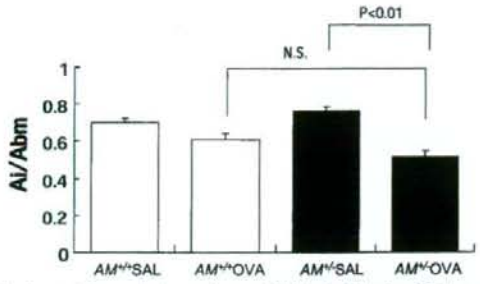

Fig. 7. Area of internal airway lumen (Ai/Abm) following OVA or SAL inhalational challenge. Ai/Abm indicates the standardized internal airway lumen area by Abm. P values are shown where significant ($P < 0.05$).

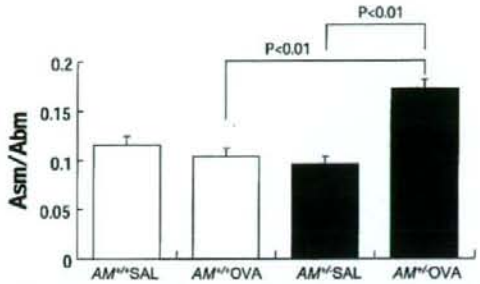

Fig. 9. Area of airway smooth muscle cell layer (Asm/Abm) following OVA or SAL inhalational challenge. Asm/Abm indicates the standardized area of airway smooth muscle cell layer by Abm. P values are shown where significant ($P < 0.05$).

may indicate that the tissue ADM expression could be enhanced by MCh challenge to protect against the airway contraction while ADM secretion of the mutant is so restricted that the mice could not react fully against MCh inhalation challenge. As a result, ADM-induced bronchodilation after MCh challenge could not occur thoroughly in the mutant. Since we found that altered ADM gene function is associated with AHR in allergen-induced asthma model, we then examined possible mechanisms of enhanced AHR in the mice.

First, we examined the roles of eosinophilic inflammation on AHR in the mice. Current experiments showed that eosinophils infiltrated markedly along the airways of the OVA-treated mice irrespective to ADM gene modulation. In asthma, a chronic inflammatory process of the airways leads to the development of airflow limitation and AHR. Extensive cellular infiltration is seen around the asthmatic airway. Particularly, airway eosinophilia is one of the most common features in asthmatic subjects and could be involved in bronchial hyperresponsiveness (5, 16). Although vasoactive peptides including ADM might affect airway inflammation after antigen challenge, our results indicate that the disruption of ADM gene has greater effects on AHR but little effect on antigen-induced airway eosinophilia in mice.

Second, we examined the potential proinflammatory mediators including immunoglobulins (OVA-specific IgE and IgG1), Th1 and Th2 cytokines, and LTs. In the current study, OVA-specific IgE in serum was not detected in each group, and the total IgE in BALF was not significantly different between the OVA-treated wild-type mice and the OVA-treated mutant mice. Th1 subtype preferentially produces IL-2, stimulating T lymphocyte proliferation, TNF-β, and IFN-γ that inhibit B lymphocyte activation and IgE synthesis. We examined IFN-γ as a Th1 cytokine, but no evidence was found suggesting its participation. Meanwhile, the OVA-specific IgG1, which is synthesized through Th1 and Th2 pathway, was not significantly suppressed in the serum of OVA-treated mutant mice. These findings indicate that the modulation of ADM gene might not affect IgE production mechanism through Th1 pathway. We also measured IL-4 and IL-5 that could evoke Th2 immune system, and no difference was found in the levels of IL-4 or IL-5 between the wild-type and the mutant animals, suggesting that the activation of Th2 pathway cannot be evoked by ADM insufficiency. Furthermore, cysteinyl LTs (LTC_4, LTD_4, and Lte_4) levels were not different between mutant mice and wild-type mice. Although cysteinyl LTs are reported to be one of the most important targets to treat bronchial asthma, they may not contribute to the AHR that is associated with ADM gene modulation.

Third, we investigated the morphological alteration of airways in the mice. Based on the fact the biochemical parameters do not primarily contribute to increase AHR in the mice, there may be another mechanism for AHR in the ADM-deficient mice. Histologically, OVA-treated airway specimen presents mucus hypersecretion involving hyperplasia of goblet cells and submucosal gland cells, which is compatible with the airways of asthmatic subjects. Therefore, goblet cell hyperplasia and associated mucus hypersecretion might be one of the important

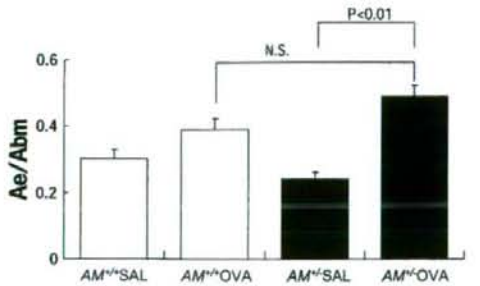

Fig. 8. Area of airway epithelial cell layer (Ae/Abm) following OVA or SAL inhalational challenge. Ae/Abm indicates the standardized area of airway epithelial cell layer by Abm. P values are shown where significant ($P < 0.05$).

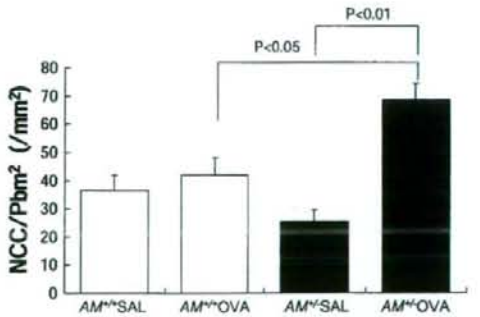

Fig. 10. NCC/Pbm^2 around the respiratory bronchioles following OVA or SAL inhalational challenge. NCC/Pbm^2 indicates the standardized nuclear cell count by Abm. P values are shown where significant ($P < 0.05$).

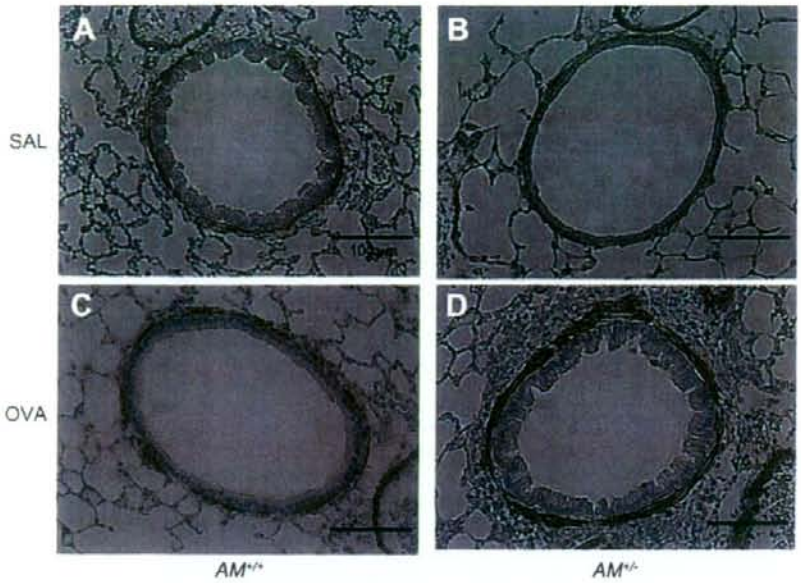

Fig. 11. Photomicrographs of small airways and lung parenchyma from saline-treated wild-type (*A*), saline-treated ADM mutant (*B*), OVA-treated wild-type (*C*), and OVA-treated ADM mutant mice (*D*) after OVA or SAL inhalational challenge. Specimens were stained with anti-α-SM actin antibody immunohistochemically. Scale bar, 100 μm.

factors of the airflow limitation and AHR in this animal model. To make this point clear, we stained each lung section by PAS and Alcian blue co-staining (PAS/Alcian blue). OVA-treated animals showed the goblet cell hyperplasia and hypersecretion as indicated by the considerable staining with PAS/Alcian blue. This phenomenon was consistently observed in the animals with OVA challenge but was not related to the ADM gene disruption, suggesting that goblet cell hyperplasia itself does not contribute the AHR in this animal model. However, our morphometric analysis data on each histological section revealed that the internal airway lumen area (Ai/Abm) of the OVA-treated mutant mice was significantly smaller than that of the OVA-untreated mutant mice. However, it was not different from that of the wild-type mice. These findings cannot endorse our physiological data that the OVA-treated mutant mice exhibit greater MCh-induced AHR. The area of airway epithelial cell layer (Ae/Abm) of the OVA-treated mutant mice was significantly larger than that of the OVA-untreated mutant mice. However, it was not different from that of the wild-type mice. Therefore, the thickening of airway epithelial cell layer cannot clearly explain greater airway responsiveness of the mutant mice.

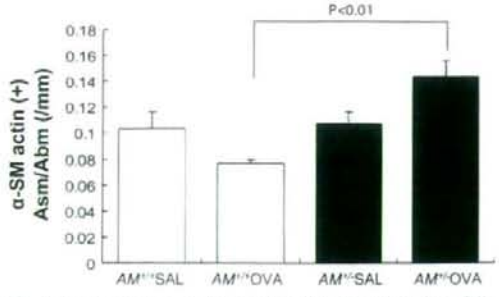

Fig. 12. Area of airway smooth muscle cell layer (Asm/Abm) following OVA or SAL inhalational challenge in the immunohistochemically stained sections with anti-α-SM actin antibody. *P* values are shown where significant ($P < 0.05$).

ADM gene is known to induce the vaso-muscle relaxation and inhibit muscle cell proliferation. The ADM gene insufficiency may be involved in the airway wall integrity in terms of cell kinetics and muscle tones. In fact, the area of the airway smooth muscle cell layer (Asm/Abm) was larger in the sensitized mutant mice than that in the sensitized wild-type mice. The peribronchial trophic changes of airway smooth muscle cells may be a primary mechanism of the current allergen-induced asthma model mice. We confirmed the ADM deficiency increases airway smooth muscle cell proliferation by using immunohistochemical staining of α-SM actin in the mouse airways. These results are consistent with the increase of nuclear cells around the basement membrane in the mice.

In this study, we did not perform an in vitro experiment concerning the effects of extracellular ADM on the airway smooth muscle proliferation. However, there are plenty of data about the inhibitory effects of ADM on smooth muscle cell proliferation in vitro and in vivo. Rossi and coworkers have demonstrated that ADM exhibits a potent dose-dependent inhibiting effect on angiotensin II (AngII)-induced human aorta smooth muscle cell proliferation and a stimulatory effect on proliferation of quiescent cells (22). Rauma-Pinola and coworkers have demonstrated that AM overexpression inhibits neointimal smooth muscle cells' growth and enhances apoptosis of the neointimal smooth muscle cells (21). It has been also reported that AM contributes to reduction of neointima formation by the inhibition of vascular smooth muscle cell proliferation via cGMP-dependent signaling pathway (1). Furthermore, ADM has an inhibitory effect on aldosterone-induced cell proliferation of adventitia in rats. This indicates that ADM may inhibit cell proliferation of both smooth muscle cells and fibroblasts in vivo (9). Consistently, it has been reported that

ADM inhibits aldosterone-induced fibroblast proliferation and ERK activity in vitro (10). Thus it may be reasonable to speculate that ADM inhibits bronchoconstrictive stress-induced cell proliferation of both smooth muscle cells and fibroblasts.

In addition, it has been reported that ADM causes the relaxation of vascular smooth muscle cells, which is associated with the intracellular cyclic AMP formation via G protein-coupled adenylate cyclase pathway (8, 14). Although the similar effects of ADM on the airway smooth muscles have not been proved yet, ADM deficiency may be associated with the less muscle relaxation through lower levels of intracellular cyclic AMP formation.

In conclusion, heterozygous ADM-deficient mice showed greater MCh-induced airway responsiveness. This is the first study that allergen-induced AHR is augmented by ADM gene disruption. Impairment of ADM gene expression does not affect airway inflammation, including eosinophilic infiltration. The airway mucus secretion, IgE synthesis, Th1 or Th2 cytokines, and cysteinyl LTs were not affected by the ADM gene modulation either. On the other hand, ADM insufficiency caused considerable airway smooth muscle hyperplasia probably due to promotion of peribronchial smooth muscle cell proliferation in the lungs. Thus ADM gene may be related to the antigen-induced airway responsiveness in association with airway smooth muscle proliferation. Furthermore, ADM might be a candidate for the novel therapeutic agent to prevent airway remodeling and asthmatic death in severe asthma. The ADM mutant mice used in this study may contribute to the study regarding the genetic roles of ADM on airway wall thickening in severe bronchial asthma and may further provide novel insights to study the physiological role of ADM in vivo.

ACKNOWLEDGMENTS

We are grateful to S. Ishii (Department of Biochemistry and Molecular Biology, Graduate School of Medicine, University of Tokyo) and T. Yokomizo (Department of Medical Biochemistry, Graduate School of Medicine, University of Kyusyu) for excellent technical assistance and valuable suggestions. We are also grateful to R. Nagai (Department of Cardiovascular Medicine, Graduate School of Medicine, University of Tokyo) for great assistance.

GRANTS

This work was supported in part by grants-in-aid for Scientific Research from the Ministry of Education, Science, Sports and Culture of Japan (no. 16590737), for the Respiratory Failure Research Group from the Ministry of Health, Labour and Welfare, Japan, and for Comprehensive Research on Aging and Health from the Ministry of Health, Labour and Welfare, Japan.

REFERENCES

1. **Agata J, Zhang JJ, Chao J, Chao L.** Adrenomedullin gene delivery inhibits neointima formation in rat artery after balloon angioplasty. *Regul Pept* 112: 115–120, 2003.
2. **Aoki-Nagase T, Nagase T, Oh-Hashi Y, Shindo T, Kurihara Y, Yamaguchi Y, Yamamoto H, Tomita T, Ohga E, Nagai R, Kurihara H, Ouchi Y.** Attenuation of antigen-induced airway hyperresponsiveness in CGRP-deficient mice. *Am J Physiol Lung Cell Mol Physiol* 283: L963–L970, 2002.
3. **Ceyhan BB, Karakurt S, Hekim N.** Plasma adrenomedullin levels in asthmatic patients. *J Asthma* 38: 221–227, 2001.
4. **Hansel NN, Diette GB.** Gene expression profiling in human asthma. *Proc Am Thorac Soc* 4: 32–36, 2007.
5. **Hogg JC.** Pathology of asthma. *J Allergy Clin Immunol* 92: 1–5, 1993.
6. **Holgate ST.** The epidemic of allergy and asthma. *Nature* 402: 2–4, 1999.
7. **Ichiki Y, Kitamura K, Kangawa K, Kawamoto M, Matsuo H, Eto T.** Distribution and characterization of immunoreactive adrenomedullin in human tissue and plasma. *FEBS Lett* 338: 6–10, 1994.
8. **Ishizaka Y, Ishizaka Y, Tanaka M, Kitamura K, Kangawa K, Minamino N, Matsuo H, Eto T.** Adrenomedullin stimulates cyclic AMP formation in rat vascular smooth muscle cells. *Biochem Biophys Res Commun* 200: 642–646, 1994.
9. **Jiang W, Yang JH, Pan CS, Qi YF, Pang YZ, Tang CS.** Effects of adrenomedullin on cell proliferation in rat adventitia induced by aldosterone. *J Hypertens* 22: 1953–1961, 2004.
10. **Jiang W, Yang JH, Wang SH, Pan CS, Qi YF, Zhao J, Tang CS.** Effects of adrenomedullin on aldosterone-induced cell proliferation in rat cardiac fibroblasts. *Biochim Biophys Acta* 1690: 265–275, 2004.
11. **Kanazawa H, Kawaguchi T, Fujii T, Kudoh S, Hirata K, Kurihara N, Takeda T.** Comparison of bronchodilator responses to adrenomedullin and proadrenomedullin N-terminal 20 peptide. *Life Sci* 57: 241–245, 1995.
12. **Kanazawa H, Kurihara N, Hirata K, Kudoh S, Kawaguchi T, Takeda T.** Adrenomedullin, a newly discovered hypotensive peptide, is a potent bronchodilator. *Biochem Biophys Res Commun* 205: 251–254, 1994.
13. **Kitamura K, Ichiki Y, Tanaka M, Kawamoto M, Emura J, Sakakibara S, Kangawa K, Matsuo H, Eto T.** Immunoreactive adrenomedullin in human plasma. *FEBS Lett* 341: 288–290, 1994.
14. **Kitamura K, Kangawa K, Kawamoto M, Ichiki Y, Nakamura S, Matsuo H, Eto T.** Adrenomedullin: a novel hypotensive peptide isolated from human pheochromocytoma. *Biochem Biophys Res Commun* 192: 553–560, 1993.
15. **Kung TT, Jones H, Adams GK 3rd, Umland SP, Kreutner W, Egan RW, Chapman RW, Watnick AS.** Characterization of a murine model of allergic pulmonary inflammation. *Int Arch Allergy Immunol* 105: 83–90, 1994.
16. **McFadden ER Jr, Gilbert IA.** Asthma. *N Engl J Med* 327: 1928–1937, 1992.
17. **McLatchie LM, Fraser NJ, Main MJ, Wise A, Brown J, Thompson N, Solari R, Lee MG, Foord SM.** RAMPs regulate the transport and ligand specificity of the calcitonin-receptor-like receptor. *Nature* 393: 333–339, 1998.
18. **Nagase T, Ishii S, Shindou H, Ouchi Y, Shimizu T.** Airway hyperresponsiveness in transgenic mice overexpressing platelet activating factor receptor is mediated by an atropine-sensitive pathway. *Am J Respir Crit Care Med* 165: 200–205, 2002.
19. **Nagase T, Matsui H, Aoki T, Ouchi Y, Fukuchi Y.** Lung tissue behavior in the mouse during constriction induced by methacholine and endothelin-1. *J Appl Physiol* 81: 2373–2378, 1996.
20. **Ohbayashi H, Suito H, Yoshida N, Ito Y, Kume H, Yamaki K.** Adrenomedullin inhibits ovalbumin-induced bronchoconstriction and airway microvascular leakage in guinea-pigs. *Eur Respir J* 14: 1076–1081, 1999.
21. **Rauma-Pinola T, Paakko P, Ilves M, Serpi R, Romppanen H, Vuolteenaho O, Ruskoaho H, Hautala T.** Adrenomedullin gene transfer induces neointimal apoptosis and inhibits neointimal hyperplasia in injured rat artery. *J Gene Med* 8: 452–458, 2006.
22. **Rossi F, Bertone C, Petricca S, Santiemma V.** Adrenomedullin antagonizes angiotensin II-stimulated proliferation of human aortic smooth muscle cells. *Peptides* 27: 2935–2941, 2006.
23. **Shindo T, Kurihara Y, Nishimatsu H, Moriyama N, Kakoki M, Wang Y, Imai Y, Ebihara A, Kuwaki T, Ju KH, Minamino N, Kangawa K, Ishikawa T, Fukuda M, Akimoto Y, Kawakami H, Imai T, Morita H, Yazaki Y, Nagai R, Hirata Y, Kurihara H.** Vascular abnormalities and elevated blood pressure in mice lacking adrenomedullin gene. *Circulation* 104: 1964–1971, 2001.

Respirology (2007) **12**, 807–813 doi: 10.1111/j.1440-1843.2007.01172.x

ORIGINAL ARTICLE

Calcitonin gene-related peptide mediates acid-induced lung injury in mice

TOMOKO AOKI-NAGASE,[1] TAKAHIDE NAGASE,[2*] YOSHIO OH-HASHI,[3] YUKIKO KURIHARA,[3] YASUHIRO YAMAGUCHI,[1] HIROSHI YAMAMOTO,[1] TAIJI NAGATA,[2] HIROKI KURIHARA[3] AND YASUYOSHI OUCHI[1]

Departments of [1]Geriatric Medicine, [2]Respiratory Medicine, and [3]Physiological Chemistry and Metabolism, Graduate School of Medicine, University of Tokyo, Tokyo, Japan

Calcitonin gene-related peptide mediates acid-induced lung injury in mice
AOKI-NAGASE T, NAGASE T, OH-HASHI Y, KURIHARA Y, YAMAGUCHI Y, YAMAMOTO H, NAGATA T, KURIHARA H, OUCHI Y. *Respirology* 2007; **12**: 807–813

Background and objective: Acid-induced lung injury from aspiration is one of the most important causes of ARDS. Calcitonin gene-related peptide (CGRP) is a neuropeptide that has various biological actions. The current study investigated whether CGRP might have pathophysiological roles in acid-induced lung injury.

Methods: The investigations employed CGRP gene-disrupted mice—mutant mice ($CGRP^{-/-}$) and their littermate controls ($CGRP^{+/+}$). Anaesthetized and mechanically ventilated mice received 2 mL/kg HCl (pH = 1.5) intratracheally. Lung wet-to-dry weight ratios were calculated to assess pulmonary oedema, total and differential cell counts of the BALF were determined, and measurements of myeloperoxidase activity were performed.

Results: Acid-induced lung injury was characterized by an increase in lung permeability and respiratory failure. Disruption of the CGRP gene significantly attenuated acid-induced injury, oedema and respiratory failure.

Conclusions: This study suggests that CGRP is involved in the pathogenesis of acute lung injury caused by acid aspiration and CGRP mutant mice may provide an appropriate model to study molecular mechanisms in this context.

Key words: acid aspiration, acute lung injury, acute respiratory distress syndrome, calcitonin gene-related peptide, knockout mice.

INTRODUCTION

ARDS is an acute lung injury, with a mortality ranging from 40% to 70% despite intensive care. Acid-induced injury from aspiration is one of the most important causes of ARDS. A potential mechanism for the acid-associated lung injury includes: (i) hydrochloric acid (HCl)-induced damage to the alveolar-capillary membrane; and (ii) polymorphonuclear neutrophil (PMN) adhesion, activation and sequestration, leading to pulmonary oedema and deterioration of gas exchange.[1,2]

Calcitonin gene-related peptide (CGRP), a 37-amino-acid peptide, is a neuropeptide that has various biological actions, including responses to sensory stimuli, cardiovascular regulation and vasodilation.[3–6] There are two CGRP isoforms, αCGRP and βCGRP. αCGRP is present in the central and peripheral nervous systems,[7] while βCGRP is expressed in specific neuronal sites.[8] In the respiratory system, CGRP is synthesized by sensory C-fibres throughout the respiratory tree[9,10] and is reported to be involved in the regulation of airway physiology.[11,12] CGRP is also found in neuroepithelial cells of the lung and coexists with tachykinins in many airway sensory nerves,[13] while CGRP receptors are found in lung vessels.[14] It has been shown that CGRP, a potent

Correspondence: Tomoko Aoki-Nagase, Department of Respiratory Medicine, Graduate School of Medicine, University of Tokyo, 7-3-1 Hongo, Bunkyo-ku, Tokyo 113-8655, Japan. Email: takahide-tky@umin.ac.jp

*Takahide Nagase, being an Associate Editor for *Respirology*, did not influence the outcome of this manuscript.

Received 11 December 2006; invited to revise 23 January 2007; revised 28 January 2007; accepted 5 March 2007 (Associate Editor: Yoichi Nakanishi).